Response to the Anonymous Referee #1

Answer to the main comments.

1.1 Anonymous Referee #1's main comments

Dear Editor:

This paper contains novel ideas about well-test analysis. In this work, the authors attempt to provide type curves for well-test analysis of fractured vertical wells at constant injection pressure using a numerical technique. Obtaining the time of termination of bilinear flow and spatiotemporal evolution of isobars are main outputs of this work. The application of the analysis proposed in this work, for instance, was shown in determination of hydraulic-fracture length. Various criteria are listed to determine the time for termination of bilinear flow; out of these criteria, reflection criterion lacks proper explanation of the mechanism for isobar reflection at fracture tip.

The authors have highlighted the advantage of well test under constant injection pressure, as it leads to almost constant well storage coefficient and it improves analysis of early-time pressure data. However, they have not clearly explained, at an early section of this manuscript, why the time of termination of bilinear flow matters from industry point of view.

The numerical technique is not explained in this manuscript. Also, to demonstrate the quality and transition of the results through various flow regimes, the authors should show a sample result of pressure contours through domain (e.g., in a 2D cross section) for a specific dimensionless fracture conductivity at various times (e.g., at three different times).

Numerous verbal and technical comments including the above shortcomings are mentioned in the attached pdf file. The authors are encouraged to edit the manuscript based on these comments and resubmit the manuscript to the editorial office.

Sincerely, Reviewer 1

1.2 Author's main response

Dear Editor:

In the first place we want to sincerely thank Anonymous Referee #1 for the detailed and extensive revision of the manuscript and for all his suggestions. They have helped us to substantially improve the manuscript and we have implemented to a large extent all the suggestions may by him.

According to the reflection criterion considered in this work, the termination of bilinear flow occurs at the time at which a first variation of pressure is evident in the fracture tip. When lower isobars than the isobar under study have already reached the fracture tip, these isobars are partly reflected from the fracture tip toward the well, due to the hydraulic conductivity contrast experienced at the interphase between the fracture tip and the matrix. This hydraulic conductivity structure causes

the isobar reflection at the fracture tip back toward the well and the isobar transmission further into the matrix. Thus, the propagation velocity of all isobars decelerates when they leave the fracture tip and start to propagate through the matrix. The previous text was added at the beginning of the section 3.2.2 “Reflection criterion”, in order to make the explanation of the criterion more understandable.

From the industry point of view, the termination time of the bilinear flow is relevant since it can be used to estimate a minimum value of fracture length when the dimensionless fracture conductivity $T_D \geq 3$. Moreover, for lower values of T_D the termination time of the bilinear flow can be used to restrict the minimum fracture length. This information is important to characterize and model a fractured reservoir. Having reliable data on fracture dimensions is critically important for production optimization strategies. The introduction was modified including this clarification as well as the corresponding cites.

In relation to a more detailed description of the numerical model, additional information has been incorporated at the beginning of section 2.4 “Description of the model setup”. This information includes the following “We ran the numerical simulations in the Subsurface Flow Module of COMSOL Multiphysics® software program. The space- and time-dependent balance equations, described in section 2.1, together with their initial and boundary conditions are numerically solved in the entire modeling domain employing the finite-element method (FEM) in a weak formulation. The discretization of the partial differential equations (PDEs) results in a large system of sparse linear algebraic equations, which are solved using the linear system solver MUMPS (MUltifrontal Massively Parallel Sparse direct Solver), implemented in the finite element simulation software COMSOL Multiphysics®. Utilizing the Galerkin approach, Lagrange quadratic shape functions have been selected to solve the discretized diffusion equations for the pressure process variable. For the time discretization, a Backward Differentiation Formula (BDF, *implicit method*) of variable order has been chosen.”. We also incorporated two important remarks concerning studies of mesh- and boundary condition-independency of the solution in the modeling domain we are most interested in. The first one “That way, boundary condition-independency of the solution has been guaranteed for in the computational subdomain of most interest” (included in the manuscript in the corresponding place), and the second one at the end of section 2.4 “We performed mesh convergence studies refining the mesh, particularly, in the computational subdomain that contains steep hydraulic gradients, until the solution became mesh-independent.”.

Additionally, in order to show the evolution of isobars we incorporated to the manuscript Figure 3 (added also to this reply), which displays simulation results of pressure contours through the computational domain in a 2D cross section for the dimensionless fracture conductivities $T_D = 0.3$ and $T_D = 6.3$ for three different times. We chose these values of T_D because they represent two interesting and illustrative scenarios. Furthermore, we introduced the following text in section 3.1 “Propagation of isobars along the fracture and the matrix”, just after the definition of P_N, “The isobars behave differently depending on the value of T_D. For cases with low T_D, it is distinguishable that after the termination of bilinear flow, the isobars reveal a tendency of progressing toward an elliptical or pseudo-radial flow while still propagating along the fracture (see, for example, $T_D = 0.3$ in Fig. 3 a, b, c). The lower the value of T_D, the more pronounced this tendency becomes. On the other hand, for high T_D the behavior of the isobars is similar to the formation linear flow beyond the fracture (see $T_D = 6.3$ in Fig. 3 d, e, f). Although the behavior of isobars after the termination of bilinear flow is also highly interesting, this aspect is not addressed in further detail in this work. It remains pending to be studied in a follow-up investigation.”.

We expose below a list with some clarifications related to the manuscript (the most important ones are discussed above) as well as some minor corrections that the Anonymous Referee #1 suggested in the supplement. With the revisions and corrections made we hope that all the questions raised by the Anonymous Referee #1 have been addressed.

Sincerely,

The authors (Patricio-Ignacio Pérez D., Adrián-Enrique Ortiz R., Ernesto Meneses Rioseco).

1.3 Author's main changes in the manuscript

1.3.1 The following text was added at the beginning of the section 3.2.2 Reflection criterion "The reflection criterion quantifies the counterclockwise deviation of type-curves from the master curve in Fig. 2 due to isobar reflection at the fracture tip (Ortiz R. et al., 2013). When lower isobars than the isobar under study have already reached the fracture tip, these isobars are partly reflected from the fracture tip toward the well, due to the hydraulic conductivity contrast experienced at the interphase between the fracture tip and the matrix. This hydraulic conductivity structure causes the isobar reflection at the fracture tip back toward the well and the isobar transmission further into the matrix. Thus, the propagation velocity of all isobars decelerates when they leave the fracture tip and start to propagate through the matrix. This criterion it is used for high dimensionless fracture conductivities:".

1.3.2 The introduction was modified including the following clarification "From the industry point of view, accurately estimating the termination time of the bilinear flow is relevant since it can be used to assess a minimum value of fracture length when the dimensionless fracture conductivity $T_D \geq 3$ (Cinco-Ley and Samaniego-V., 1981). To underpin the latter, Ortiz R. et al. (2013) demonstrated that for T_D approximately higher than 10 the fracture half-length can be estimated as $x_F = C(D_b t_{ebl})^{1/4}$, where C is a constant, D_b is the bilinear hydraulic diffusivity, and t_{ebl} the termination time of the bilinear flow. Moreover, for lower values of T_D the termination time of the bilinear flow can be used to restrict the minimum fracture length. This information is important to characterize and model a fractured reservoir. Having reliable data on fracture dimensions is critically important for production optimization strategies.".

1.3.3 The following information has been incorporated at the beginning of section 2.4 Description of the model setup " We ran the numerical simulations in the Subsurface Flow Module of COMSOL Multiphysics® software program. The space- and time-dependent balance equations, described in section 2.1, together with their initial and boundary conditions are numerically solved in the entire modeling domain employing the finite-element method (FEM) in a weak formulation. The discretization of the partial differential equations (PDEs) results in a large system of sparse linear algebraic equations, which are solved using the linear system solver MUMPS (MUltifrontal Massively Parallel Sparse direct Solver), implemented in the finite element simulation software COMSOL Multiphysics®. Utilizing the Galerkin approach, Lagrange quadratic shape functions have been selected to solve the discretized diffusion equations for the pressure process variable. For the time discretization, a Backward Differentiation Formula (BDF, *implicit method*) of variable order has been chosen.".

1.3.4 We incorporated the following remark in the corresponding place of section 2.4 Description of the model setup "That way, boundary condition-independency of the solution has been guaranteed for in the computational subdomain of most interest.".

1.3.5 We incorporated the following remark at the end of section 2.4 Description of the model setup "We performed mesh convergence studies refining the mesh, particularly, in the computational subdomain that contains steep hydraulic gradients, until the solution became mesh-independent.".

1.3.6 We incorporated to the manuscript Figure 3. Due to the addition of Fig. 3 to the manuscript, the numbering of the subsequent figures as well as the references related to the concerned figures throughout the manuscript has been consequently shifted.

1.3.7 We introduced the following text in section 3.1 "Propagation of isobars along the fracture and the matrix", just after the definition of P_N, "The isobars behave differently depending on the value of T_D. For cases with low T_D, it is distinguishable that after the termination of bilinear flow, the isobars reveal a tendency of progressing toward an elliptical or pseudo-radial flow while still propagating along the fracture (see, for example, $T_D = 0.3$ in Fig. 3 a, b, c). The lower the value of T_D, the more pronounced this tendency becomes. On the other hand, for high T_D the behavior of the isobars is similar to the formation linear flow beyond the fracture (see $T_D = 6.3$ in Fig. 3 d, e, f). Although the behavior of isobars after the termination of bilinear flow is also highly interesting, this aspect is not addressed in further detail in this work. It remains pending to be studied in a follow-up investigation.".

Answer to the relevant comments in the supplement.

As suggested by the journal's guidelines, only the most relevant comments are addressed here. Further minor comments can be read in the authors answer to the Anonymous Referee #1's comments, previously uploaded to the interactive webpage. We want to indicate, however, that all changes made to the manuscript regarding the minor comments are displayed in the marked-up version of the manuscript.

2.1 Anonymous Referee #1's comment, P1L11 of the old version of the manuscript.

Injection wells in operation usually do not work under constant pressure. They operate at specified injection rates. The authors should clarify about the operational mechanism that the constant-pressure injection is feasible. If there is not enough operational insights about this condition, the authors should limit this constant-pressure condition to producing wells.

2.2 Author's response

You are right, in most cases operational injection wells work under constant flow rate. However, our investigation aims at contributing to a better understanding of the evaluation and interpretation of transient flow rate curves and pressure diffusion in fractured reservoirs for both producing wells and well tests. Some well tests are performed under a constant pressure condition, they have the advantage of minimizing changes in the wellbore storage coefficient (Earlougher Jr., 1977).

2.3 Author's change in the manuscript

Accordingly, the first sentence of the abstract was modified to "This work studies intensively the flow in fractures with finite hydraulic conductivity intersected by a well injecting/producing at constant pressure, either during an injection/production well test or the operation of a production well.".

3.1 Anonymous Referee #1's comment, P2L63 of the old version of the manuscript.

At constant-pressure boundary condition? Please be clear about what conditions lead to no analytical solution for the pressure diffusion equation.

3.2 Author's response

There is no analytical solution for the pressure diffusion equation when considering the case of injecting/producing water to/from a vertical fracture embedded in a matrix by means of a well.

3.3 Author's change in the manuscript

Accordingly, in the manuscript the sentence was modified to "Conceivably, one of the main reasons why constant pressure tests is not a more common technique in reservoir engineering arises from the fact that no analytical solutions are available for the pressure diffusion equation when considering injection/production at constant pressure in fractured geologic media (Kutasov and Eppelbaum, 2005)."

4.1 Anonymous Referee #1's comment, P8L229 of the old version of the manuscript.

What does "acceleration" mean here? The authors must clarify about its meaning in the manuscript.

4.2 Author's response

We have considered the classic definition of acceleration, which is the rate of change of velocity with respect to time.

4.3 Author's change in the manuscript

The previous statement was added to the manuscript (in the corresponding place) in order to clarify the meaning of acceleration.

5.1 Anonymous Referee #1's comment, P8L234 of the old version of the manuscript.

Figure 5 contradicts with the statement that the higher the isobar, the sooner it migrates. For instance, consider a specific time (e.g., 10^-8). Isobar 0.66 reaches to x_iD of 0.02 whereas isobar 0.01 reaches to x_iD of 0.2. This shows that isobar 0.01 is faster than isobar 0.66. Please revise the relevant statements to clarify this contradiction.

5.2 Author's response

Considering the case you exposed related to Fig. 5 (now Fig. 6 in the new version of the manuscript), the isobar 0.66 reaches the grey line at $x_{iD} = 0.02$ and at $\tau = 5 \cdot 10^{-10}$, and the isobar 0.01 reaches the grey line at $x_{iD} = 0.2$ and at $\tau = 2 \cdot 10^{-9}$. We can see that the isobar 0.66 (in terms of time) reaches the grey line earlier than the isobar 0.01. This means that the isobar 0.06 starts to behave according to the bilinear flow behavior earlier than the isobar 0.01. That is what we mean in the sentence **"**when discussing qualitatively about the early time we notice that the higher the value of the isobar P_N the sooner it migrates proportional to the fourth root of time (Fig. 6)". We do not state that the higher the value of isobar the faster it is,

we state that the higher the isobar the sooner it starts to behave according to bilinear flow, that is propagating along the fracture proportional to the fourth root of time. However, after reading the sentence more carefully we find that the word combination "sooner it migrates" may be misleading.

5.3 Author's change in the manuscript

To make it clearer, we slightly reformulated the sentence into "when discussing qualitatively about the early time we notice that the higher the value of the isobar $\boldsymbol{P_N}$ the sooner it starts behaving proportional to the fourth root of time (Fig. 6)".

6.1 Anonymous Referee #1's comment, P10L275 of the old version of the manuscript.

According to Fig. 2, the terms 1/q_wDt and 2.60tau^1/4 should be replaced with log(1/q_wDt) and log(2.60tau^1/4) because Fig. 2 is in log-log plot.

6.2 Author's response

We followed your recommendation.

6.3 Author's change in the manuscript

We corrected the equation accordingly. This was also carried out for all concerned cases.

7.1 Anonymous Referee #1's comment, P10L276 of the old version of the manuscript.

Not defined in the paper. The term in Fig. 2 is q_wD not q_wDt.

7.2 Author's response

As you say, Fig. 2 is a graph showing $1/q_{wD}$ vs. τ for different dimensionless fracture conductivities. The curves describing the behavior of the reciprocal of dimensionless flow rate over time for different dimensionless fracture conductivities, from $T_D = 0.1$ up to $T_D = 100$, are referred to as type-curves (black lines in Fig. 2). We invoke the behavior of q_{wD} for the different type-curves as q_{wDt}. The latter is the term we compare to the master curve (in the case of reflection criterion) or the bilinear-fit-curve (in the case of transition criterion) through the definition of the criteria.

7.3 Author's change in the manuscript

To clarify this, the following sentence has been now added to the manuscript "where q_{wDt} represents the dimensionless flow rate q_{wD} of the specific type-curve under study (Fig. 2)".

8.1 Anonymous Referee #1's comment, P10L283 of the old version of the manuscript.

At infinity? What is infinity here?

8.2 Author's response

When we referred to "infinity", we meant by that "an infinitely long fracture"

8.3 Author's change in the manuscript

We reformulated the concerned sentence to "where $q_{wD\infty}$ denotes the dimensionless flow rate of the master curve (Fig. 2), which describes the behavior for the case of an infinitely long fracture.". We hope now that this way the doubt has been removed.

9.1 Anonymous Referee #1's comment, P10L284 of the old version of the manuscript.

This must be tau_t not tau_r, and different from the parameter in the following parentheses.

9.2 Author's response

τ_t represents the *termination time* of the bilinear flow regime when the transition criterion is used to identify the time at which bilinear flow ends. Analogously, τ_r represents the *termination time* when the reflection criterion is utilized to determine the time at which the bilinear flow regime culminates. Consequently, since we are presenting the reflection criterion, we must use τ_r within the parentheses. Please see also the next answer to the next comment.

9.3 Author's change in the manuscript

This answer does not lead to any change in the manuscript.

10.1Anonymous Referee #1's comment, P10L284 of the old version of the manuscript.

According to Fig. 7, the high T_D, the shorter the reflection time (tau_r; box symbols) not termination time (tau_t; circle symbols). tau_t is almost constant with change of T_D.

10.2Author's response

The terminology *termination time* is generally involved in every criterion that aims at identifying the end of the bilinear flow regime. This terminology (*termination time*) is a general way to refer to the time at which bilinear flow ceases and it is not attributed to any specific criterion. For instance, the transition time τ_t and reflection time τ_r represent the *termination time* of bilinear flow, but for different ranges of T_D.

10.3Author's changes in the manuscript

10.3.1 To avoid confusion to the reader, we changed *termination time* to "transition time" in section 3.2.1, *termination time* to "reflection time" in section 3.2.2, *termination time* to "arrival time" in section 3.2.3, and *termination time* to "fracture time" in section 3.2.4.

10.3.2 Additionally, we added the following sentence in the introductory part of section 3.2 "It is noteworthy that the termination time is referred to differently, according to the criterion used to identify the time at which the bilinear flow regime ceases (e.g. transition time τ_t, reflection time τ_r, arrival time τ_a, and fracture time τ_F, introduced in the subsections 3.2.1, 3.2.2, 3.2.3, and 3.2.4, respectively).".

11.1Anonymous Referee #1's comment, P10L288 of the old version of the manuscript.

A criterion is a conditional statement which determines a condition upon satisfaction of the equality in a criterion. Because of that, Eq. 22 in this section must be an inequality such as epsilon>0. Provided that epsilon>0, bilinear flow switches to radial flow. Right?
Please clarify all above criteria (reflection criterion, transition criterion) following this comment.

11.2Author's response

As you raise the question, it may be expected to be radial flow, but it may be elliptical or pseudo-radial as well. In our investigation we did not go deeper to prove it, thus we cannot confirm it.

11.3Author's changes in the manuscript

11.3.1 We followed your advice of substituting "=" by "<" in the epsilon definitions in the respective criteria.

11.3.2 The following explanation was added at the end of the introductory part of section 3.2 "Further, criteria generally aim at defining the deviation of curves obtained by numerical simulations from analytical fit curves that correspond to bilinear flow. The deviation is quantified by introducing the quantity ε (see subsections 3.2.1, 3.2.2, and 3.2.4). That is, the numerical results differ from the analytical bilinear fit curves by a value of ε due to the transition to another flow regime. Throughout the manuscript we use, for instance, $\varepsilon = 0.01$ or $\varepsilon = 0.05$ corresponding to 1% and 5% deviation, respectively. This employed notation is intended to express that when a separation between numerical results and fit curves is greater than 1% or 5%, the termination of bilinear flow is evidenced.". We hope now that this contributes to a better understanding of the epsilon definitions in the criteria and the use of epsilon values throughout the manuscript.

12.1Anonymous Referee #1's comment, P12L337 of the old version of the manuscript.

A deceleration? Figs. 3g-j show that the isobars decelerate once they reach the fracture tip.

12.2Author's response

We recognize that the statement used is not clear in English and therefore we reformulated it, hoping that it is now clear what we mean. In Figs. 3g-j (now Figs. 4g-j in the new version of the manuscript) we refer to the increase of velocity just before the isobars arrives at the fracture tip, what correspond to an acceleration. The latter was demonstrated in the last part of section 3.1 "Propagation of the isobars along the fracture and the matrix".

12.3Author's change in the manuscript

We rephrased the words concerned and now we write the following "at times shortly before the isobars reach the fracture tip". We went through the manuscript and whenever this previous "confusing phrase" was present we corrected accordingly.

13.1Anonymous Referee #1's comment, P12L362 of the old version of the manuscript.

What epsilon is this one? There are three definitions of epsilon in Eqs. 20-22.

13.2Author's response

When we use the expression ε and $P_N = 0.01$, it means that we are studying the case of the isobar $P_N = 0.01$ and we are considering that for values of ε greater than 0.01, the bilinear flow ends. In the concerned sentence we are referring to Fig. 7a (now Fig. 8a in the new version of the manuscript), where the four criteria presented in this manuscript play a role. Therefore, this epsilon is related to the relevant criteria exhibiting a value of 0.01 according to their respective definitions (Eq. 20 – 22). It is important to note that only one criterion can be fulfilled at a time. In Fig. 7b (now Fig. 8b in the new version of the manuscript), we consider ε and $P_N = 0.05$, that is we are studying the isobar $P_N = 0.05$ and we are using a value of $\varepsilon = 0.05$ to determine the termination of bilinear flow, for all pertinent criteria.

13.3Author's changes in the manuscript

13.3.1 To make it more understandable for the reader, we incorporated the following clarification in the introductory part of section 3.2 "It is important to mention that only one criterion can be fulfilled at a time".

13.3.2 We incorporated the following clarification in the corresponding place (right after Eq. 24) "It is worth noting that when using the expression ε and $P_N = 0.01$, it means that we are studying the case of the isobar $P_N = 0.01$ and we are considering that for values of ε greater than 0.01, the bilinear flow ends. Note further that when considering ε and $P_N = 0.05$, we are studying the isobar $P_N = 0.05$ and we are using a value of $\varepsilon = 0.05$ to determine the termination of bilinear flow, for all pertinent criteria." .

14.1Anonymous Referee #1's comment, P13L364 of the old version of the manuscript.

Not clear. Explain more with magnifying the area of interest out of Fig. 7 for this statement.

14.2Author's response

In order to clarify this, we modified the concerned sentence. We now hope that this new statement better explains this striking feature observed in Fig. 7a and Fig. 7b (now Fig. 8a and Fig. 8b in the new version of the manuscript), within the considered ranges. That said, we further hope that magnifying the areas in the graphs, where this feature is exposed, is no longer necessary. We believe that magnifying the area will not give substantial information to the reader.

14.3Author's change in the manuscript

In order to clarify this, we modified the concerned sentence to "Note that for the case ε and $P_N = 0.01$ and $2 < T_D < 3$ (see Fig. 8a), it is observed that values (non-filled circles) depart from the fit-curve linked to the transition criterion and start converging toward the fit-curve associated with the reflection criterion. A similar behavior is also observed for the case ε and $P_N = 0.05$ and $1.1 < T_D < 2$ (see Fig. 8b). A comprehensive study is required to unravel more precisely what occurs within those ranges of T_D. Based on their work, Ortiz R. et al. (2013) came to the same conclusion.".

Response to the Anonymous Referee #2

Anonymous Referee #2's comment

"This paper investigates the flow in a fracture from an injection well into a confined reservoir. The paper seeks for a numerical solution to be compared with an analytical solution already existed. To me the paper does not have a novelty and as written does not add additional value. The authors have previously published a similar paper on the subject: "Two-dimensional numerical investigations on the termination of bilinear flow in fractures" by Ortiz and Renner 2013."

Author's response

Dear Editor:

We are grateful to the Anonymous Referee #2 for his devoted time and his feedback, which allows us to enhance the quality of our manuscript and clarify some observations made by the Referee #2. In particular, we want to thank the Anonymous Referee #2 also for his relatively negative opinion, which may have originated from a series of misunderstandings while reading the manuscript. That motivated and encouraged us to make some points in the manuscript even clearer so that such possible misunderstandings are avoided. In the following we want to clear up those misunderstandings.

A.1 Anonymous Referee #2's statement

"The paper seeks for a numerical solution to be compared with an analytical solution already existed".

A.2 Author's response

The comparison between the numerical simulation result with the semi-analytical (not analytical) solution proposed by Guppy et al. (1981b) was performed solely with the objective of verifying that our numerical model was well set. Subsequently, by using (i) the validated numerical solution and (ii) different methodologies, we were able to produce novel results that are presented and documented for the first time in our work for the case of constant pressure in the well. As explained below, it is important to strengthen the point that the numerical experiments conducted in this study and the extent of the analyses performed go far beyond the study of the transient flow rate done by Guppy et al. (1981b).

A.3 Author's change in the manuscript

This answer does not lead to any change in the manuscript.

B.1 Anonymous Referee #2's statement

"To me the paper does not have a novelty and as written does not add additional value".

B.2 Author's response

Since it may be the case that the novelty of our present work has not been clearly highlighted in the manuscript, we present the new findings of this work for the case of injecting/producing at constant pressure in the well:

i. In this work, we present for the first time for the case of injection/production at constant pressure in the well the equation describing the spatiotemporal evolution of the isobars along the fracture during the bilinear flow regime (Eq. 16).

ii. In this study, expressions are presented for the first time that quantitatively identify the termination time of bilinear flow when injecting/producing at constant pressure into/from the fracture. The criteria used to quantitatively identify the termination of bilinear flow are explained in detail in sections 3.2.1, 3.2.2, 3.2.3, and 3.2.4. In this work two methodologies are employed to detect the termination of bilinear flow under constant pressure conditions in the well: (a) considering the transition of flow rate in the well and (b) considering the propagation of isobars P_N along the fracture (highlighted in section 3.2 "Termination of bilinear flow").

iii. In this investigation, a new methodology is exposed to constrain the fracture length, based on the end time of the bilinear flow and using the Eq. 16 that describes the spatiotemporal evolution of the isobars along the fracture during the bilinear flow regime (see section 4.1).

iv. In this manuscript, an expression is presented for the first time that allows to determine the time at which a specific isobar arrives at the fracture tip. In terms of dimensionless parameters, this expression is dependent only on T_D (see section 3.2.3 and τ_a in Fig. 7 of the manuscript version read by the Referee #2).

v. A study is conducted for the first time in this work with the purpose of analyzing the velocity of the isobars along the fracture, aiming at distinguishing that the isobars experience an acceleration shortly before they arrive at the fracture tip, which differs from their previous behavior (see end of section 3.1).

The comments made by the Referee #2 encouraged us to carry out an extensive and detailed revision of the manuscript. We acknowledge that the novelty of the results and the key points in our work might have not been highlighted enough in the old version of the manuscript. Therefore, we highlighted the most significant findings of this work in the conclusion section, making it clearer what the novelty of this work is.

B.3 Author's change in the manuscript

The conclusion section has been restructured and reformulated in the new version of the manuscript as follows:

"Numerical results obtained in this work corroborated the relation of proportionality previously presented by Guppy et al. (1981b) between the reciprocal of dimensionless flow rate $1/q_{wD}$ and the fourth root of dimensionless time τ during the bilinear flow regime for the case of injection/production at constant pressure in the well. Guppy et al. (1981b) obtained the proportionality factor $A = 2.722$ (Eq. 10), which is slightly greater than the factor obtained here $A = 2.60$ (Eq. 12). This discrepancy may be attributed to our finer spatial and temporal discretization in comparison with the discretization used by Guppy et al. (1981b).
The most significant findings of this work are:

i) During the bilinear flow regime, the migration of isobars along the fracture is described as: $x_i(t) = \alpha_b (D_b t)^{1/4}$, where $D_b = T_F^2 / k_m \eta_f s_m$ ($m^4 s^{-1}$) is the effective hydraulic diffusivity of fracture during the bilinear flow regime. In addition, the migration of isobars in the matrix is given by: $y_i(t) = \alpha_m (D_m t)^{1/2}$, where $D_m = k_m/(\eta_f s_m)$ ($m^2 s^{-1}$) denotes the hydraulic diffusivity of matrix. This simulation results are in line with the study conducted by Ortiz R. et al. (2013) for the case of wells injecting/producing at constant flow rate.

ii) The termination of bilinear flow obtained from transient flow rate analysis is given by (a) the transition time τ_t (circumferences in Fig. 8 and Eq. 20), valid for low T_D and (b) the reflection time τ_r (squares in Fig. 8 and Eq. 21), valid for high T_D.

iii) From the physical point of view, it is of interest to study the propagation of isobars along the fracture, for which the termination of bilinear flow has been found in this work to be given by (a) the fracture time τ_F (filled circles in Fig. 8 and Eq. 22), valid for low T_D and (b) the arrival time τ_a (triangles in Fig. 8), valid for high T_D. However, this methodology may encounter technological obstacles in real field situations.

iv) A new methodology is presented to constrain the fracture length (section 4.1), based on the end time of the bilinear flow and using Eq. (16) that describes the spatiotemporal evolution of the isobars along the fracture during the bilinear flow regime.

v) In terms of dimensionless parameters, the time at which a specific isobar arrives at the fracture tip is dependent only on T_D (see section 3.2.3 and τ_a in Fig. 8).

Similarly as in Ortiz R. et al. (2013), it is observed that the isobars exhibit a peak of acceleration shortly before they arrive at the fracture tip (Figs. 4 and 6). This acceleration was verified by studying the velocity of isobars using the graphs v_{iD} vs. τ and v_{iD} vs. x_{iD} (Fig. 7). It was concluded that for a fixed dimensionless position in the fracture x_{iD}, the velocity v_{iD} is higher for lower values of normalized isobars p_N as well as for higher dimensionless fracture conductivities T_D (see Figs. 7b and 7d).

In a follow-up study, it would be interesting to include the effect of fracture storativity and investigate, utilizing an analogue method to that discussed in this work, the behavior of a fracture with conductivity high enough to lead to fracture and formation linear flow."

C.1 Anonymous Referee #2's statement

"The authors have previously published a similar paper on the subject: "Two-dimensional numerical investigations on the termination of bilinear flow in fractures" by Ortiz and Renner 2013.".

C.2 Author's response

Although, the present work uses some of the methodologies presented by Ortiz R. et al. (2013), the present work considers, among other aspects, a different study case. Ortiz R. et al. (2013) studied the behavior of the bilinear flow regime in a fracture and matrix formation injecting/producing at constant flow rate in the well, whereas we investigate in the present work the case of injecting/producing at constant pressure in the well. In addition, we want to clarify that only one of the present authors published the article cited by the Referee #2.

Our work constitutes a complement and a further development of the work previously published by Ortiz R. et al. (2013).

C.3 Author's change in the manuscript

Despite the fact that we refer to the previous work conducted by Ortiz R. et al. (2013) in the introduction section while addressing the state of the art in the topic in question, we additionally refer to the study of Ortiz R. et al. (2013) in the new version of this manuscript by adding the following sentence in the introduction, in the line 106 of the manuscript version read by the Referee #2: "Some of the methodologies used in this work are inspired by the study conducted by Ortiz R. et al. (2013) for wells operating at constant flow rate (pressure transient analysis)".

1.1.1 Anonymous Referee #2's statement

"The problem statement is very simplified.".

1.1.2 Author's response

This observation may have derived from the Referees #2's assumption that the authors did not use a dual-porosity dual-permeability model. As we explain later, the general formulation of the physical problem in question is performed using a dual-porosity dual-permeability approach (see few lines below). Further, we use a fit-for-purpose model and with the aim of investigating the behavior of isobars along a fracture with finite conductivity, the model captures the main physical processes and reliably represents reservoir structure and property distribution (dual-porosity dual-permeability).

1.1.3 Author's change in the manuscript

This answer does not lead to any change in the manuscript.

1.2.1 Anonymous Referee #2's statement

"Numerical solutions already exist"

1.2.2 Author's response

To the best of our knowledge, only a semi-analytical solution for the transient well flow rate exists when imposing a constant pressure in the well, which has been presented by Guppy et al. (1981b). No numerical investigation has been documented for (i) the study of the advancement of isobars along the fracture and (ii) the termination time of bilinear flow, when operating with constant pressure in the well. We want to emphasize that finding a numerical solution to be compared with a semi-analytical solution documented by Guppy et al. (1981b) does not constitute the main purpose of our investigation. This comparison was performed only with the purpose of corroborating that our numerical experimental design was well posed. Subsequently, by using the validated numerical solution we were able to produce the novel results mentioned previously in this letter.

We carefully revised each publication mentioned by the Referee #2. It is correct that all these investigations seek for analytical or semi-analytical solutions, however, with the exception of Guppy et al. (1981b), none of them consider the problem statement with a constant pressure in the well. As mentioned earlier, the semi-analytical solution documented by

Guppy et al. (1981b) was used in our work solely to validate the numerical solution obtained using the simulation software COMSOL Multiphysics.

We kindly ask the Referee #2 to have a look at the further remarks 1-2 included at the end of this reply.

1.2.3 Author's change in the manuscript

This answer does not lead to any change in the manuscript.

2.1 Anonymous Referee #2's comment

"Use of a reservoir simulator is recommended than COMSOL. Please check the literature on numerical solutions of reservoir simulations. Numerical solutions using reservoir simulations provide additional options necessary for this work: dual-porosity dual-permeability models. Authors might be able to use Comsol porous media flow module. However, there might be more updates in reservoir simulations packages. I checked the underlying equations and there is no porosity or indication of porous medium. A dual-porosity dual-permeability model must be used in this case. Similar research using this approach: Dejam, M., Hassanzadeh, H. and Chen, Z., 2018. Semianalytical solution for pressure transient analysis of a hydraulically fractured vertical well in a bounded dual-porosity reservoir. Journal of hydrology, 565, pp.289-301."

2.2 Author's response

We want to clarify that we did not use "Comsol Porous Media Flow Module". The Comsol Multiphysics module we used is "Subsurface Flow Module", which includes groundwater flow in porous and fractured geologic media. This is clearly stated in our manuscript (see section 2.4 of the new version of the manuscript). For further details we kindly ask the Referee #2 to have a look at:

i. COMSOL Multiphysics Reference Manual, version 5.4, COMSOL, Inc, www.comsol.com

ii. Subsurface Flow Module User's Guide, version 5.4, COMSOL, Inc, www.comsol.com. Chapter 3 *Porous Media and Subsurface Flow Interfaces*, and specially Subchapter *The Darcy's Law Interface* and Subchapter *The Fracture Flow Interface*.

It is worth noting that dual-porosity dual-permeability models set up in COMSOL Multiphysics have been successfully tested, validated and benchmarked in numerous published works (e.g. Shao et al. 2014).

We agree with the Referee #2 that for the question at hand one must use a dual-porosity dual-permeability model and so we did indeed in our work. We kindly encourage the Referee #2 to carefully read the Eqs. (1) and (2) (see k_m (m^2) and T_F (m^3)), where we explicitly consider two permeabilities, one for the matrix formation and one for the fracture.

As for porosity of the matrix rock and the fracture, these are considered in the respective diffusivity equations (Eqs. 1 and 2, respectively). In our work, porosity is implicitly included in the respective specific storage capacity for the matrix and the fracture (s_m (Pa^{-1}) and s_F (Pa^{-1}), see Eqs. 1 and 2, respectively). The value of s_m (Pa^{-1}) used in our work is documented in section 2.4 and the value of s_F (Pa^{-1}) is neglected since the fracture is considered nondeformable and the amount of fluid in the fracture is considered small enough to consider its compressibility as negligible. In addition, the porosity of the fracture

is negligible in comparison to the porosity of the matrix. The pressure in the fracture is dictated by an inhomogeneous diffusivity equation, which contains a time-dependent source term $q_F(x,t)$ but it does not involve an intrinsic transient term. The storativity or more precisely the storage coefficient depends on porosity of rock and compressibility of fluid and rock. We kindly ask the Referee #2 to have a look at:

- Singhal and Gupta 2010, Chapter 8 *Hydraulic Properties of Rocks*, and specifically Eqs. 8.11 and 8.12, as well as Subchapter 8.2.1 *Relationship of Hydraulic Conductivity with Fracture Aperture and Spacing*, Eq. 8.15.

- Maliva 2016, Chapter 1 *Aquifer Characterization and Properties*, and specially Subchapter 1.4.3 *Storativity*.

- Bear 2007, Chapter 5 *Mathematical Statement of the Groundwater Forecasting Problem*, and more precisely Subchapter 5.1 *Aquifer Storativity* and Subchapter 5.2 *Basic Continuity Equation*, Eqs. 5.20 – 5.29.

- Bear and Cheng 2010, Chapter 5.1 *Mass Balance Equations*, and particularly Subchapter 5.1.2 *Deformable Porous Medium* and Subchapter 5.1.3 *Specific Storativity*, Eqs. 5.1.30 – 5.1.32 and Eqs. 5.1.47 – 5.1.50; to mention a few.

In particular, we kindly ask the Referee #2 to have a look at the following link for the physical and numerical formulation of dual-porosity dual-permeability model in COMSOL Multiphysics:

- https://www.comsol.com/model/discrete-fracture-691

For the formulation of the groundwater flow equation (so-called "diffusivity equation"), which is a result of the combination of the impulse (Darcy equation) and mass (continuity equation) balance equations, in terms of the storage coefficient we kindly ask the Referee #2 to have a look at:

- Singhal and Gupta 2010, Subchapter 7.1.3 *General Equation of Flow*, Eqs. 7.19-7.25, Subchapter 19.5 *Modeling of Homogeneous Porous Aquifer*, Eqs. 19.1, 19.3 and 19.4.

- Bear 2018, Chapter 5 *Modeling Single-Phase Mass Transport*, and specifically Subchapter 5.3.1 *Deriving 2-D Balance Equations by Integration*, A. *Confined Aquifer*, Eqs. 5.3.26 – 5.3.33.

- Bear 2007, Chapter 5 *Mathematical Statement of the Groundwater Forecasting Problem*, and more precisely Subchapter 5.1 *Aquifer Storativity* and Subchapter 5.2 *Basic Continuity Equation*, Eqs. 5.20 – 5.29.

- Bear and Cheng 2010, Chapter 5.1 *Mass Balance Equations*, and in particular Subchapter 5.1.4 *Flow equations*, Eqs. 5.1.73 – 5.1.76.

- To mention a few.

In reservoir engineering, it is more typical for the transient diffusivity equation to be given explicitly in terms of porosity of the formation and compressibility of fluid and rock. In groundwater hydraulics and hydrogeology, it is more common to express the transient diffusivity equation in terms of the storage coefficient as we did in our work.

That said, we want to point out that dual-porosity dual-permeability models have been successfully mathematically modelled and simulated using the simulation software COMSOL Multiphysics (e.g. Shao et al. 2014 and references therein). As for the mathematical physics, as described in section 2.1, in our work the dual-porosity dual-permeability model, implemented in COMSOL Multiphysics, is examined by considering the diffusivity equation for the rock matrix and for the fracture (Eqs. 1 and 2, respectively), each containing their respective permeability and porosity (read above) parameters (k_m (m^2), T_F (m^3) and s_m (Pa^{-1}), s_F (Pa^{-1})). The coupling between the two equations is given by the term $q_F(x,t)$ (Eq. 4), which expresses the mass exchange between fracture and matrix. We hope that it is now clear that the general formulation of our numerical model is expressed in terms of a dual-porosity dual-permeability approach.

We kindly ask the Referee #2 to have a look at the further remarks 3-7 included at the end of this reply.

Please note that all the references of this answer are included at the end of this reply.

2.3 Author's changes in the manuscript

2.3.1 We added in the new version of the manuscript the following clarifying statement right before Eq. (3) "In addition, the porosity of the fracture is negligible in comparison to the porosity of the matrix. Note, however, that the pressure in the fracture is dictated by an inhomogeneous diffusivity equation, which contains a time-dependent source term $q_F(x,t)$ but it does not involve an intrinsic transient term.".

2.3.2 To avoid possible misunderstandings and make this point even clearer in the new version of the manuscript, we rephrased the second sentence of the beginning of section 2.1 "governing equations and parameters". Now we write in the revised manuscript "In a general formulation of a dual-porosity dual-permeability model, the equation utilized to describe the hydraulics of single-phase compressible Newtonian fluid in a reservoir matrix is given by:". Additionally, right after the presentation of Eq. (1) and when referring to the storage coefficient, we write the following "It is worth noting that the storage coefficient depends on porosity of rock and compressibility of fluid and rock". The Referee #2 will be able to see these clarifications in the revised version of the manuscript. We hope now that this fundamental misunderstanding is cleared up.

3.1 Anonymous Referee #2's comment

"The effect of boundary condition can be investigated by changing the boundary condition from close to open and even partially open boundary condition instead of changing the size of the domain. The effect of boundary condition must be investigated. The termination of bilinear flow and transition to boundary dominated flow is dictated by the boundary. It is recommended to change the boundary condition for a specific domain and analyze the results or investigate the effect of distance to a closed boundary on the results."

3.2 Author's response

We agree with the Referee #2 that the effect of boundary condition must be investigated. There are different ways to conduct such study. As explained in the manuscript version read by the Referee #2, we performed such a study of the effect of boundary condition on the simulation results. For the concrete model described in the present work, we chose the method of enlarging the modeling domain size until a boundary-condition-independent simulation outcome was observed. That is, the boundaries of the model were set far enough that the chosen boundary condition (no-flow) had no impact on the simulation results.

The Referee #2 proposed to study the effect of boundary conditions by changing them from close to open reservoir. We followed Referee #2's suggestion since it represents another way of proving that in our model the boundary conditions do not affect the results for the interested simulation time. We see here an opportunity to make this point clearer and avoid misunderstandings.

In Fig. 1 of this answer (see at the end of this response) we show a similar graph to that used in the manuscript to study the behavior of the reciprocal of flow rate in the well vs. time (Fig. 2 in the manuscript). We find this graph appropriate to investigate the influence of changing the boundary condition from no-flow to constant pressure ($p = 100\ kPa$, equal to the initial condition in the fracture-matrix system). In this work, we studied a range of T_D from 0.1 up to 100, therefore we accordingly chose the following three representative examples: T_D = 0.3, 6.3 and 50. We can see in Fig. 1 of this reply that we obtain the same simulation results when considering no-flow or constant pressure boundary condition for the simulation time considered in our investigation. Thus, boundary condition-independency of the simulation results is guaranteed for the simulation time considered in our numerical experiments. In Fig. 1 of this reply the termination time of bilinear flow, which is the time window of most interest from the entire simulation time for this work, for the case of $T_D = 50$, 6.3 and 0.3 is $\tau_r = 3.86 \times 10^{-8}$, $\tau_r = 1.69 \times 10^{-4}$, and $\tau_t = 1.78 \times 10^{-2}$, respectively. It is worth noting that the termination time of bilinear flow regime is identified by the deviation of the respective type-curves from the bilinear-fit-curve.

Alternatively, for the case of no-flow boundary condition considered in the present work, monitoring the pressure at the boundaries of the model constitutes another way of studying the effects of the imposed boundary condition on the simulation results. If the pressure at the boundaries does not change during the entire simulation time considered, this means more evidently that the boundary condition does not affect the modeling outcomes. We additionally conducted such a study for three selected points at the boundaries of the modeling domain (see Figs. 2 and 3 of this answer, at the end of this response). We were able to observe that the pressure does not change, representing this a strong indication that the no-flow boundary condition set does not affect the simulation results.

We now hope that the study of the effect of different boundary conditions on the simulation results is clarified. We offer to include these additional studies in the supplement of the online version of the paper. Furthermore, we offer to upload the data related to the model setup and simulation results obtained with COMSOL Multiphysics to provide the interested reader with the possibility of testing and verifying the model.

3.3 Author's change in the manuscript

3.3.1 The following sentence was added to the manuscript in the corresponding place of section 2.4 Description of the model setup "Additional studies have been conducted to further examine the independency of simulation results from the boundary conditions set for the simulation time considered. The pressure has been monitored at the boundary of the model for the case of imposing no-flow boundary condition (closed reservoir). No pressure variation has been detected at the boundaries of the model, which corroborates the previous observation that the simulation results have not been affected by the boundary condition set. Further, the boundary condition has been changed to constant pressure (open reservoir). Also, for this latter case, no changes were recognized in the simulation results."

We hope that all the questions raised by the Anonymous Referee #2 have been addressed.

Sincerely,

The authors (Patricio-Ignacio Pérez D., Adrián-Enrique Ortiz R., Ernesto Meneses Rioseco).

Further remarks of the answer (Anonymous Referee #2):

1. Had our proposed model been oversimplified, we would not have been able to validate our numerical results with the semi-analytical solution suggested by Guppy et al. (1981b) for the bilinear flow regime. As demonstrated in our work, as a first step we validated our numerical results with the semi-analytical solution introduced by Guppy et al. (1981b) for the bilinear flow regime.

2. Had our proposed model not considered flow in fractured and porous media (dual permeability model), it would not have been possible to obtain bilinear flow. As it has been proven in our work, we were able to numerically simulate bilinear flow regime.

3. Validated physical models that credibly simulate physical reservoir processes such as groundwater flow in fractured porous media with COMSOL Multiphysics have been successfully documented and published in international, peer-review journals (see item 5. below). From the point of view of the authors, what matters is a rigorously formulated, mathematically validated simulator that reliably represents the physics of the reservoir processes. As a matter of example: tested, benchmarked and generally validated reservoir models, including a variety of coupled reservoir processes have been simulated with COMSOL Multiphysics, e.g:

- https://www.comsol.de/blogs/modeling-geothermal-processes-comsol-software/

We kindly ask the Referee #2 to have a look at a large list of validated models in different research fields that have been simulated with COMSOL Multiphysics and the corresponding published literature on the following link (COMSOL Verification and Validation Models):

- https://www.comsol.com/verification-models/?sort=popularity

In addition, we kindly ask the Referee #2 to check an extensive literature on published works, documenting modeling and simulation of reservoir processes with COMSOL Multiphysics on the following link:

- https://www.comsol.de/papers-presentations

(Relevant contributions can be filtered by the Referee #2 by entering the concerned keywords).

Multiphysics is certainly one of the strengths of COMSOL. Rigorously modeling and simulating the multiphysical nature of reservoir processes in fractured porous geologic media constitutes one of the strengths of COMSOL Multiphysics. Slightly different PDEs, e.g. for heat and solute transport, are coupled with the flow equations, both in porous and fractured geologic media.

4. Alternatively, and/or additionally, benchmarking our model has been an important step to show that the simulation software COMSOL Multiphysics is suitable. Generally speaking, various sources for benchmarking fracture-flow can be found e.g.:

- https://git.iws.uni-stuttgart.de/benchmarks/fracture-flow

(see also “Benchmarks for single-phase flow in fractured porous media" by B. Flemisch et al. 2017).

As mentioned previously, as a first step we have corroborated our numerical results concerning the bilinear flow regime with the semi-analytical solution suggested by Guppy et al. (1981b).

5. Further, we kindly encourage the Referee #2 to check numerous published works in reservoir engineering that address flow in fractures and matrix formation using COMSOL Multiphysics as reservoir simulator:

https://www.onepetro.org/search?q=COMSOL+Multiphysics&peer_reviewed=&published_between=&from_year=&to_year=&rows=25

(COMSOL Multiphysics as keyword).

The robustness of the simulation software COMSOL Multiphysics for groundwater flow in fractured porous media has been shown in several works published in international and peer-reviewed journals, e.g.:

- Zhang, Q., Ju, Y., Gong, W., Zhang, L., Sun, H.: Numerical simulations of seepage flow in rough single rock fractures, Petroleum, Vol. 1, Issue 3, pp. 200-205, https://doi.org/10.1016/j.petlm.2015.09.003, 2015.

- Qu, Z.-q., Zhang, W., Guo, T.-k.: Influence of different fracture morphology on heat mining performance of enhanced geothermal systems based on COMSOL, International Journal of Hydrogen Energy, Vol. 42, Issue 29, pp. 18263 – 18278, https://doi.org/10.1016/j.ijhydene.2017.04.168, 2017.

- Wang, L., Cardenas, M. B., Slottke, D. T., Ketcham, R. A., Sharp, J. M.: Modification of the Local Cubic Law of fracture flow for weak inertia, tortuosity, and roughness, Water Resources Research, 51, pp. 2064–2080, https://doi.org/10.1002/2014WR015815, 2015.

- Chen B., Song E., Cheng X.: Plane-Symmetrical Simulation of Flow and Heat Transport in Fractured Geological Media: A Discrete Fracture Model with Comsol, In: Laloui L., Ferrari A. (eds) Multiphysical Testing of Soils and Shales, Springer Series in Geomechanics and Geoengineering, Springer, Berlin, Heidelberg, https://doi.org/10.1007/978-3-642-32492-5_17, 2013.

- Saeid, S., Al-Khoury, R., Barends, F.: An efficient computational model for deep low-enthalpy geothermal systems, Computers & Geosciences, 51, pp. 400 – 409, https://doi.org/10.1016/j.cageo.2012.08.019, 2013.

- Ekneligoda, Th. Ch. & Min, K.-B.: Determination of optimum parameters of doublet system in a horizontally fractured geothermal reservoir, Renewable Energy, 65, pp. 152 – 160, https://doi.org/10.1016/j.renene.2013.08.003, 2014.

- Kristinof, R., Ranjith, P.G. & Choi, S.K.: Finite element simulation of fluid flow in fractured rock media, Environ Earth Sci, 60, pp. 765–773, https://doi.org/10.1007/s12665-009-0214-2, 2009.

- Li, Q., Ito, K. Wu, Z., Lowry, Ch. S., Loheide, S. P.: COMSOL Multiphysics: A Novel Approach to Ground Water Modeling, Ground Water, Edi. Zheng, Ch, Vol. 47, No. 4, https://doi.org/10.1111/j.1745-6584.2009.00584.x, 2009.

- To mention a few.

6. Other reservoir simulators widely used in academics and industry for one-phase, compressible groundwater flow in saturated, confined aquifers, that use the same formulation for the description of flow in fractures and formation matrix in terms of the storage coefficient as COMSOL Multiphysics, are FEFLOW® (developed by DHI WASY) and MODFLOW (developed by the USGS) – to mention a few. We kindly ask the Referee #2 to have a look at, e.g.:

- Diersch 2014, Chapter 9 *Flow in Saturated Porous Medium: Groundwater Flow*, and more specifically Subchapter 9.2.1 *Basic Equations*, Eqs. 9.1 – 9.2; and Chapter 4 *Discrete Features*. (Diersch, H.-J.G.: FEEFLOW: Finite Element Modeling of Flow, Mass and Heat Transport in Porous and Fractured Media, Springer Science + Business Media B.V., https://doi.org/10.1007/978-3-642-38739-5, 2014.)

-https://www.usgs.gov/mission-areas/water-resources/science/modflow-and-related-programs?qt-science_center_objects=0#qt-science_center_objectsc and the documentation for the MODFLOW 6 Groundwater Flow Model (Chapter 55 of Section A, *Groundwater*, Book 6 *Modeling Techniques*, Eq. 2-2, https://pubs.usgs.gov/tm/06/a55/tm6a55.pdf).

- Vázquez-Báez, V., Rubio-Arellano, A., García-Toral, D., Rodríguez-Mora, I.: Modeling an Aquifer: Numerical Solution to the Groundwater Flow Equation, Mathematical Problems in Engineering, Vol. 2019, Article ID 1613726, https://doi.org/10.1155/2019/1613726, 2019.

- Kumar, C. P. & Singh, S.: Concepts and Modeling of Groundwater System, International Journal of Innovative Science, Engineering & Technology – IJISET, Vol. 2, issue 2, 2015.

7. Although the Referee #2 suggests using another reservoir simulator where the diffusivity equation for transient flow is explicitly expressed in terms of porosity and compressibility and where dual-porosity dual permeability models can also be designed, no concrete reservoir simulator is proposed by the Referee #2. In case more commercial reservoir simulators, perhaps more widely used in petroleum engineering for multi-phase flow of black oil and gas such as MultiSim™ and Schlumberger Eclipse are meant, we want to refer to the strengths and limitations of those simulation software. We kindly ask the Referee #2 to have a look at, e.g.:

- Chin, W. C. & Zhuang, X. 2020, Chapter 3 *Reservoir Simulation – Strengths, Limitations and Strategies*. (Chin, W. C. & Zhuang, X.: Reservoir Simulation and Well Interference: Parent-child, Multilateral Well and Fracture Interactions, Handbook of Petroleum Engineering, Scrivener Publishing LCC, First Edition by John Wiley & Sons, Inc, 2020.)

- EGL Eclipse Reservoir Simulation Software, Eclipse Reference Manual, Version 2018.1.

The strengths and limitations of different simulation software for fluid flow in fractured porous geologic media are attributed to numerous aspects, such as: Assumption and approximations in the mathematical physics considered, implementation of the specific numerical method used (FDM, FEM, VEM, etc...), space and time discretization algorithms, mesh generator capabilities (Cartesian, rectangular or curvilinear coordinates), linearization techniques, stabilization, convergence, speed, visualization techniques, test, validation, etc...). It is beyond the scope of our answer to compare several reservoir simulators in terms of their strengths and limitations.

Although some industries claim to have developed "All-purpose", "comprehensive" reservoir simulators, for every application there are several reservoir simulators revealing advantages and disadvantages. Every simulation study (experiment design) of fluid flow in fractured porous media constitutes a unique series of actions, initiating from the aquifer characterization to the ultimate examination of results. We kindly ask the Referee #2 to have a look at, e.g.:

- Islam, M. R., Hossain, M. E., Moussavizadegan, S. H., Mustafiz, S., Abou-Kassem, J. H.: Advanced Petroleum Reservoir Simulation: Towards Developing Reservoir Emulators, Second Edition, Scrivener Publishing LLC, Co-published by John Wiley & Sons, Inc. Hoboken, New Jersey, 2012.

- Chin, W. C.: Reservoir Engineering in Modern Oilfields: Vertical, Deviated, Horizontal and Multilateral Well Systems, Handbook of Petroleum Engineering Series, Vol.1, Scrivener Publishing LCC, Co-published by John Wiley & Sons, Inc. Hoboken, New Jersey, 2016.

- Chin, W. C. & Zhuang, X.: Reservoir Simulation and Well Interference: Parent-child, Multilateral Well and Fracture Interactions, Handbook of Petroleum Engineering, Scrivener Publishing LCC, First Edition by John Wiley & Sons, Inc, 2020.

References of the answer (Anonymous Referee #2):

1. Singhal, B. B. S. and Gupta, R. P.: Applied Hydrogeology of Fractured Rocks, Second Edition, Springer Science + Business Media B.V., https*://doi*.org*/10.1007/978-90-481-8799-7*, 2010.

2. Maliva, R. G.: Aquifer Characterization Techniques, Schlumberger Methods in Water Resources Evaluation, Series No. 4, *c*, Springer International Publishing Switzerland, https*://doi*.org*/10.1007/978-3-319-32137-0*, 2016.

3. Bear, J. and Cheng A. H.-D.: Modeling Groundwater Flow and Contaminant Transport, *Theory and Applications of Transport in Porous Media*, Springer Science + Business Media B.V., https*://doi*.org*/10.1007/978-1-4020-6682-5*, 2010.

4. Bear, J.: Hydraulics of Groundwater, Manufactured in the United States of America Dover Publications Inc., 31 East 2nd Street, Minoela, N.Y. 11501, 2007.

5. Bear, J.: Modeling Phenomena of Flow and Transport in Porous Media, *Theory and Applications of Transport in Porous Media*, Edi. Hassanizadeh, S. M. Springer International Publishing AG, https*://doi.org/10.1007/978-3-319-72826-1*, 2018.

6. Shao, W., Bogaard, T., Bakker, M.: How to Use COMSOL Multiphysics for Coupled Dual-Permeability Hydrological and Slope Stability Modeling, Procedia Earth and Planetary Sciences, 9, 83-90, https://doi.org/10.1016/j.proeps.2014.06.018, 2014.

Figures of the answer (Anonymous Referee #2):

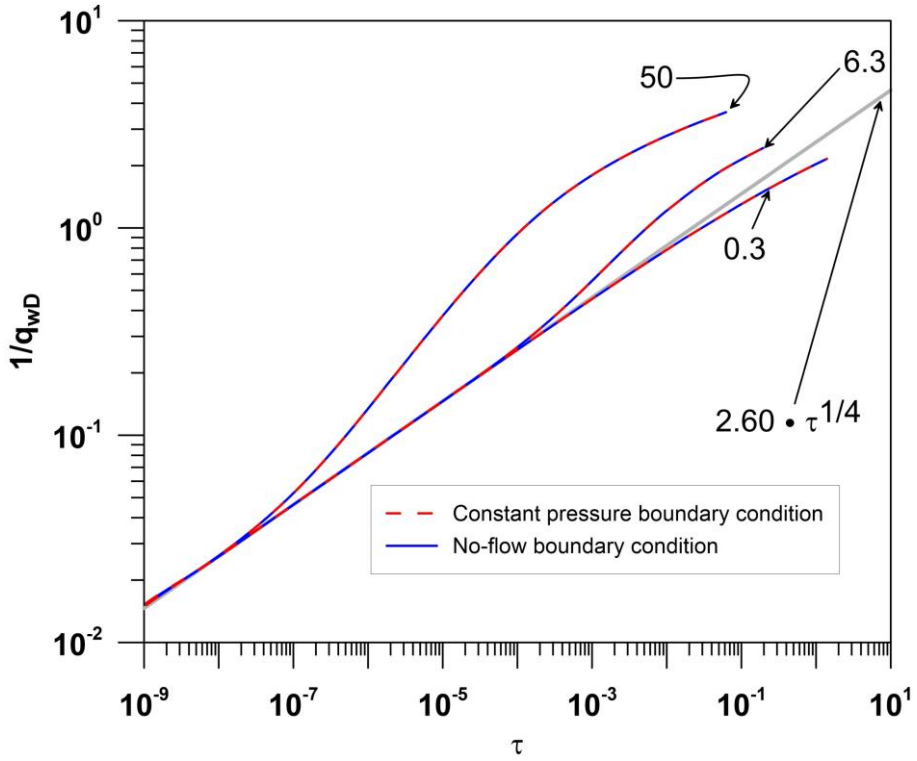

Figure 1: Model results displayed as $1/q_{wD}$ vs. τ in log-log scale. Bilinear-fit-curve (grey line) and type-curves for different boundary conditions: no-flow and constant pressure.

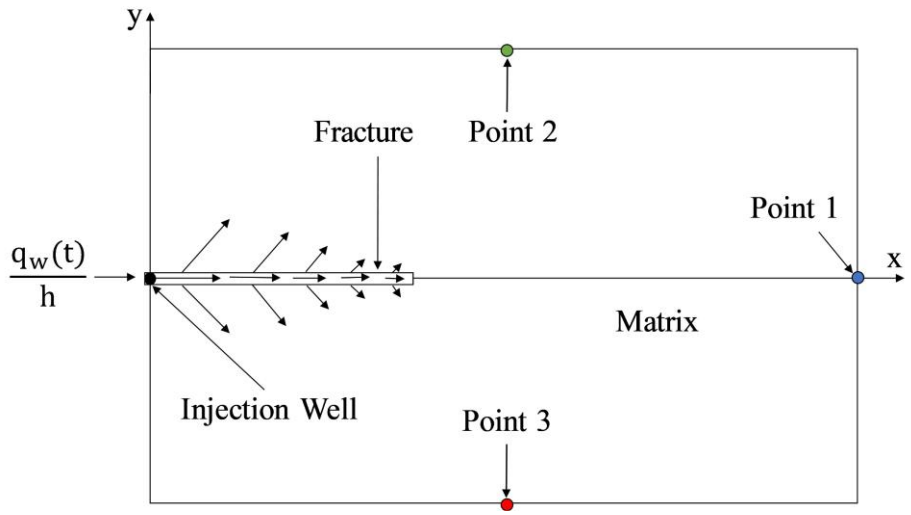

Figure 2: Representation of the main features of the model (not scaled). Note the 3 points at the boundaries of the model where the pressure was monitored during the simulation time (see Fig. 3 of this reply).

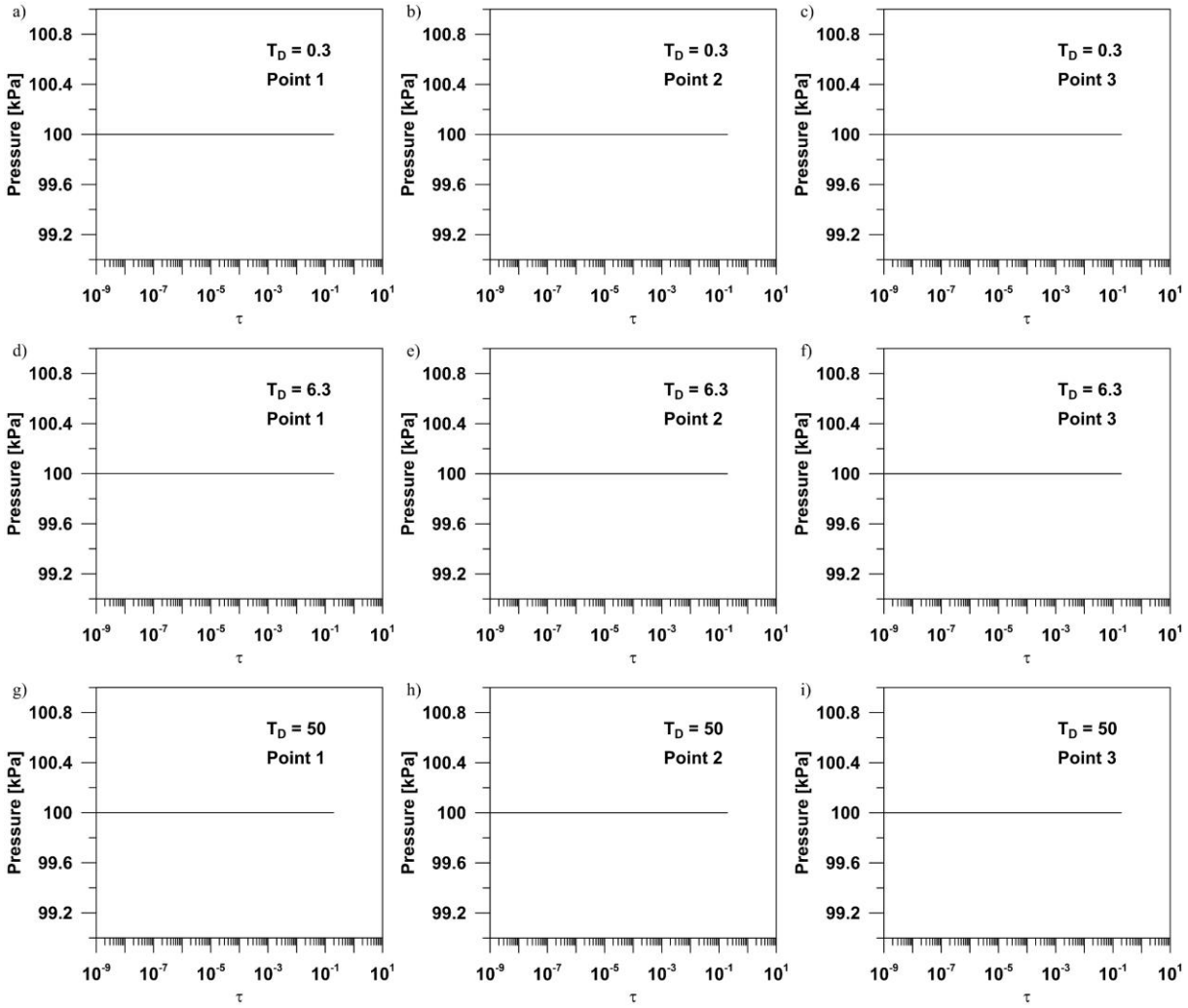

Figure 3: Monitored pressure at three different points located at the boundaries of the model (see Fig. 2 of this reply) for three representative cases of T_D displayed in Fig. 1 of this reply, when imposing no-flow boundary condition.

965

970

Bilinear pressure diffusion and termination of bilinear flow in a vertically fractured well injecting at constant pressure

Patricio-Ignacio Pérez D.[1], Adrián-Enrique Ortiz R.[2], Ernesto Meneses Rioseco[3,4]

[1]Department of Mechanical Engineering, Universidad Técnica Federico Santa María, Valparaíso, 2340000, Chile
[2]Department of Chemical and Environmental Engineering, Universidad Técnica Federico Santa María, Valparaíso, 2340000, Chile
[3]Department of Geothermics and Information Systems, Leibniz Institute for Applied Geophysics, Hannover, 30655, Germany
[4](Currently at) Department Subsurface Use, Federal Institute for Geosciences and Natural Resources, Hannover, 30655, Germany

Correspondence to: Adrián-Enrique Ortiz R. (adrian.ortiz@usm.cl)

Abstract. ~~This work studies intensively the flow in fractures with finite hydraulic conductivity intersected by a well injecting/producing at constant pressure~~ This work studies intensively the flow in fractures with finite hydraulic conductivity intersected by a well injecting/producing at constant pressure, either during an injection/production well test or the operation of a production well. Previous investigations showed that for a certain time the reciprocal of flow rate is proportional to the fourth root of time, which is characteristic of the flow regime known as bilinear flow. Using a 2D numerical model, we demonstrated that during the bilinear flow regime the transient propagation of isobars along the fracture is proportional to the fourth root of time. Moreover, we present relations to calculate the termination time of bilinear flow under constant injection or production well pressure, as well as, an expression for the bilinear hydraulic diffusivity of fractures with finite hydraulic conductivity. To determine the termination of bilinear flow regime, two different methods were used: (a) numerically measuring the transient ~~of~~ flow rate in the well and (b) analyzing the propagation of isobars along the fracture. Numerical results show that for low dimensionless fracture conductivities the transition from bilinear flow to another flow regime (e.g. pseudo-radial flow) occurs before the pressure front reaches the fracture tip and for high dimensionless fracture conductivities it occurs when the pressure front arrives at the fracture tip. Hence, this work complements and advances previous research on the interpretation and evaluation of well test analysis under different reservoir conditions. Our results aim at improving the understanding of the hydraulic diffusion in fractured geologic media and as a result they can be utilized for the interpretation of hydraulic tests, for example to estimate the fracture length.

Keywords: Bilinear flow; Rate transient analysis; Hydraulic diffusivity; Pressure diffusion; Porous and fractured geologic media.

Highlights

- The reciprocal of flow rate is proportional to the fourth root of time.
- The migration of isobars in the fracture is proportional to the fourth root of time.

- For low dimensionless fracture conductivities, bilinear flow ends before the pressure front reaches the fracture tip.
- For high dimensionless fracture conductivities, bilinear flow ends when the pressure front reaches the fracture tip.
- Isobars accelerate when they approach to the fracture tip.

1 Introduction

Understanding the different flow regimes in fractured reservoirs has always been key in the interpretation and evaluation of hydraulic well tests as well as in the production optimization of reservoirs. An in-depth description of the behavior of multiple flow regimes in fractures is extremely important to master the physics behind the modeling and simulation and, hence, to reliably interpret the results. Models considering a double porosity were first examined by Barenblatt et al. (1960). They introduced the basics of fluid dynamics in fissured rocks by deriving general equations of the seepage of liquid in porous media, taking into consideration its double-porosity condition. Cinco-Ley and Samaniego-V. (1981) differentiated clearly four flow regimes: fracture linear flow, bilinear flow (for the first time named in this way by them), formation linear flow, and pseudo-radial flow.

Usually, reservoir properties are obtained from well test or production data at a constant flow rate (pressure transient analysis). However, in ~~some~~most cases, reservoir production is performed at a constant pressure. This is illustrated, for instance, by the case where fluid is produced from the reservoir by means of a separator or constant-pressure pipeline (e.g., gas wells; Ehlig-Economides, 1979). Open wells flow at constant atmospheric pressure, e.g., artesian water wells. Geothermal fluid production may propel a back-pressure steam turbine, where steam leaves the turbine at the atmospheric pressure or at a higher constant pressure. Other operational conditions that require to maintain a constant pressure are encountered in gas wells, where a fixed pressure must be maintained for sales purposes or in water injection wells, where the injection pressure is constant (Da Prat, 1990). In addition, reservoir production at constant pressure is conducted during rate decline periods of reservoir depletion (Da Prat, 1990; Ehlig-Economides, 1979). Although the interpretation of data collected in well tests and production at constant flow rate (pressure transient analysis) has considerably improved, the rate transient analysis has not experienced such development (Houzé et al., 2018). Lately, a significant interest for the rate transient analysis has increased, which is attributed to the exploitation of unconventional hydrocarbon plays due to the extremely slow and long transient responses (Houzé et al., 2018). The production from unconventional plays has recently been made possible by creating fractures, which has strengthened the importance of having better tools and methods that allow to obtain information of the fractures considering either the transient analysis of pressure or flow rate or the combination of both. It is exceedingly difficult to maintain a constant flow rate during long times, especially in low permeability formations as in the case of unconventional plays (Kutasov and Eppelbaum, 2005). It is worth mentioning that constant-pressure tests have the advantage of minimizing changes in the wellbore storage coefficient (Earlougher Jr., 1977). The wellbore storage effects distort early-time pressure evolution, subsequently, the constant-pressure well tests allow the analysis of early-time data and in this way information of the reservoir in the vicinity of the wellbore can be obtained

(Nashawi and Malallah, 2007). Moreover, rate-transient tests are particularly suitable for the illustration of the long-term behavior of formations (Torcuk et al., 2013). ~~Conceivably one of the main reasons why constant pressure tests is not a more common technique in reservoir engineering arises from the fact that in some cases no analytical solutions are available for the pressure diffusion equation (Kutasov and Eppelbaum, 2005).~~ Conceivably, one of the main reasons why constant pressure tests is not a more common technique in reservoir engineering arises from the fact that no analytical solutions are available for the pressure diffusivity equation when considering injection/production at constant pressure in fracture geologic media (Kutasov and Eppelbaum, 2005).

Arps (1945) presented an empirical production correlation for the rate history of a well during the boundary-dominated flow regime. Later, Locke and Sawyer (1975) generated type-curves for a vertically fractured reservoir producing at constant pressure with the objective of characterizing the behavior of flow rate. In this context, Agarwal et al. (1979) presented type-curves to analyze the early time cases. In addition, they determined the dimensionless fracture conductivity T_D by means of graphing the logarithm of the reciprocal of flow rate vs. the logarithm of time and utilizing type-curve matching techniques. Fetkovich (1980) introduced the rate decline analysis in the radial-flow system, similar to pressure transient analysis, however, only applicable to circular homogeneous reservoirs.

Guppy et al. (1981a) studied the effect of non-Darcy flow within a fracture. They concluded that the dimensionless fracture conductivity T_D ~~has~~can be expressed as an apparent conductivity that is not constant over time. Subsequently, a major contribution was made by Guppy et al. (1981b), which consisted of presenting semi-analytical solutions for bilinear flow~~,—~~ both works considered constant pressure production. They demonstrated that the reciprocal of dimensionless flow rate is proportional to the fourth root of dimensionless time when producing at constant wellbore pressure. Guppy et al. (1988) contributed further to the previous works investigating deeply the cases with turbulent flow in the fracture and for the first time they examined a technique that concerns both buildup and drawdown data when the well is producing at constant pressure. Subsequently, a direct method to estimate the turbulent term considering high-velocity flow in variable rate tests was documented by Samaniego-V. and Cinco-Ley (1991). In addition, Berumen et al. (1997) developed a transient pressure analysis under both constant wellhead and bottom-hole pressure conditions considering high-velocity flow. Wattenbarger et al. (1998) presented decline curve analysis methods for tight gas wells producing at constant pressure with long-term linear behavior (fracture flow). Pratikno et al. (2003) prepared rate-time decline curves for fractured wells producing at constant pressure, including fracture lineal and bilinear flow. Follow-up investigations conducted by Nashawi (2006) presented semi-analytical solutions when considering non-Darcy flow in a fracture and a method with which it is possible to quantify the turbulence in a fracture. Nashawi and Malallah (2007) developed a direct method to determine the fracture and reservoir parameters without having to use type-curve matching techniques. In this context, Heidari Sureshjani and Clarkson (2015) concluded that plotting techniques overestimate the fracture half-length, leading them to the formulation of an analytical methodology with which ~~it~~ the fracture half-length is estimated more precisely.

Recently, Silva-López et al. (2018) introduced a new method to obtain Laplace-transform~~ed~~ solutions, and as a result, they predicted new regions of flow behavior. This latter method is documented for injecti on~~ng~~ at either constant flow rate or

pressure. In addition, the theory of well testing has been improved by investigating the effects of non-uniform properties of hydraulic fractures (He et al., 2018). Moreover, Wang et al. (2018) presented an enhanced model to simulate the productivity of volume fractured wells and Dejam et al. (2018) documented a new semi-analytical solution applicable in dual-porosity ~~formations~~ formulations.

When it comes to studying the termination of bilinear flow regime and the spatiotemporal propagations of isobars, there is not much evidence of investigations considering injection or production at constant pressure. To the best of our knowledge, it has only been investigated when injecting at constant flow rate in the well (Cinco-Ley and Samaniego-V., 1981; Weir, 1999). In this regard, new criteria to determine the end of bilinear flow, which are also used in this investigation, were introduced by Ortiz R. et al. (2013). From the industry point of view, accurately estimating the termination time of the bilinear flow is relevant since it can be used to assess a minimum value of fracture length when the dimensionless fracture conductivity $T_D \geq 3$ (Cinco-Ley and Samaniego-V., 1981). To underpin the latter, Ortiz R. et al. (2013) demonstrated that for T_D approximately higher than 10 the fracture half-length can be estimated as $x_F = C(D_b t_{ebl})^{1/4}$, where C is a constant, D_b is the bilinear hydraulic diffusivity, and t_{ebl} the termination time of the bilinear flow. Moreover, for lower values of T_D the termination time of the bilinear flow can be used to restrict the minimum fracture length. This information is important to characterize and model a fractured reservoir. Having reliable data on fracture dimensions is critically important for production optimization strategies.

This work addresses the challenging task of gaining a quantitative understanding of bilinear flow from rate transient analysis for wells producing at constant pressure, requiring a multidisciplinary approach. Expanding the understanding of bilinear flow regime in fractured reservoirs leads to a more precise analysis of well tests and production or injection data. This, in turn, makes it possible to characterize a reservoir more accurately and consequently have more reliable assessments of its behavior, leading to better concepts of production optimization during operation. Some of the methodologies used in this work are inspired by the study conducted by Ortiz R. et al. (2013) for wells operating at constant flow rate (pressure transient analysis).

Taking into account injection at constant pressure, this investigation presents for the first time: (a) the propagation of isobars P_N along the fracture and the formation during bilinear flow regime, as well as the computation of the bilinear hydraulic diffusivity of fracture; and (b) the study of termination of bilinear flow regime utilizing criteria previously presented and a criterion firstly documented here.

2 Background

2.1 Governing equations and parameters

~~This study is carried out considering that single-phase fluid in both matrix and fracture obeys the Darcy's law in a two-dimensional confined and saturated aquifer. The selected software simulator for numerically modeling groundwater flow in~~

~~the reservoir is COMSOL Multiphysics. For the matrix, the equation utilized to describe the hydraulics of compressible Newtonian fluid in a fractured reservoir is given by:~~ This study is carried out considering that single-phase fluid in both matrix and fracture obeys the Darcy's law in a two-dimensional confined and saturated aquifer. In a general formulation of a dual-porosity dual-permeability model, the equation utilized to describe the hydraulics of a single-phase compressible Newtonian fluid in a reservoir matrix is given by:

$$s_m \frac{\partial p}{\partial t} = \frac{k_m}{\eta_f}\left(\frac{\partial^2 p}{\partial x^2} + \frac{\partial^2 p}{\partial y^2}\right), \quad (1)$$

where s_m (Pa^{-1}) represents the specific storage capacity of matrix, k_m (m^2) the matrix permeability, η_f (Pa s) the dynamic fluid viscosity, and p (Pa) the fluid pressure. It is worth noting that the storage coefficient depends on porosity of rock and compressibility of fluid and rock. For the fracture, the equation is given by:

$$s_F b_F \frac{\partial p}{\partial t} = \frac{T_F}{\eta_f}\frac{\partial^2 p}{\partial x^2} + \frac{q_F(x,t)}{h}, \quad (2)$$

where s_F (Pa^{-1}) represents the specific storage capacity of fracture, b_F (m) the aperture of fracture, T_F (m^3) the fracture conductivity, h (m) the fracture height, and $q_F(x,t)$ the fluid flow between matrix and fracture (see Cinco L. et al., 1978 and Guppy et al., 1981b). In this study, s_F is neglected because we assume that the fracture is non-deformable and the amount of fluid in the fracture is small enough to consider its compressibility as negligible. In addition, the porosity of the fracture is negligible in comparison to the porosity of the matrix. Note, however, that the pressure in the fracture is dictated by an inhomogeneous diffusivity equation, which contains a time-dependent source term $q_F(x,t)$ but it does not involve an intrinsic transient term. Thus, Eq. (2) reads:

$$\frac{T_F}{\eta_f}\frac{\partial^2 p}{\partial x^2} + \frac{q_F(x,t)}{h} = 0. \quad (3)$$

The pressure diffusivity~~on~~ equations for matrix and fracture are coupled by the term $q_F(x,t)$, which is defined as:

$$\frac{q_F(x,t)}{h} = 2\frac{k_m}{\eta_f}\frac{dp}{dy}\Big|_{y=0}, \quad (4)$$

where the factor 2 relates to the contact between matrix and fracture via its two surfaces.

2.2 Dimensionless parameters

This study is conducted using dimensional properties, but the analysis of results is performed utilizing the conventional dimensionless definitions. The dimensionless flow rate is given by:

$$\frac{1}{q_{wD}} = \frac{k_m h(p_w - p_i)}{q_w \eta_f}, \quad (5)$$

where q_w ($m^3\,s^{-1}$) represents the flow rate in the well, q_{wD} the dimensionless flow rate in the well, h (m) the fracture height, p_i (Pa) the initial pressure of the formation and fracture, and p_w (Pa) the constant injection pressure.

The dimensionless fracture conductivity is defined as:

$$T_D = \frac{T_F}{k_m x_F}, \tag{6}$$

~~where $T_F = k_F b_F$ (m^3) denotes the fracture conductivity and x_F (m) the fracture half-length.~~ where $T_F = k_F b_F$ (m^3) denotes the fracture conductivity, x_F (m) the fracture half-length, and k_F (m^2) the fracture permeability. Note that T_D is the same as $(k_f b_f)_D$ used in Cinco-Ley and Samaniego-V. (1981) or F_{CD} used in Gidley et al. (1990).

Instead of using the conventional definition of dimensionless time $t_D = tD_m/{x_F}^2$, we prefer to use a modified definition presented by Ortiz R. et al. (2013):

$$\tau = \frac{t_D}{{T_D}^2} = \frac{D_m {k_m}^2}{{T_F}^2} t, \tag{7}$$

where $D_m = k_m/(\eta_f s_m)$ (m^2 s^{-1}) represents the hydraulic diffusivity of matrix and τ the dimensionless time. Finally, the dimensionless x-coordinate, which corresponds to the fracture axis (see Fig. 1), is defined as:

$$x_D = \frac{x}{x_F}; \tag{8}$$

and the dimensionless y-coordinate, that represents the axis perpendicular to the fracture (see Fig. 1), is defined as:

$$y_D = \frac{y}{x_F}. \tag{9}$$

2.3 Previous solutions for bilinear flow at constant wellbore pressure

As mentioned earlier, bilinear flow regime was firstly documented by Cinco-Ley and Samaniego-V. (1981). According to their proposed definition, it consists of an incompressible linear flow within the fracture and a slightly compressible linear flow in the formation. Moreover, a semi-analytical solution for a vertically fractured well producing at constant pressure during bilinear flow regime was presented by Guppy et al. (1981b). They demonstrated that the reciprocal of flow rate is proportional to the fourth root of time and the governing equation is given in dimensionless form by:

$$\frac{1}{q_{wD}}(\tau) = \frac{\pi \Gamma(3/4)}{\sqrt{2T_D}} {t_D}^{1/4} \cong 2.722\tau^{1/4}. \tag{10}$$

where $\Gamma(3/4)$ represents the gamma function evaluated in $3/4$. Silva-López et al. (2018) presented an analytical solution for an infinite fracture considering the case of variable flow rate for long-time in dimensionless form:

$$\frac{1}{q_{wD}}(t_D) = \frac{1}{f(t_D)} \frac{\pi^{1/4}\sqrt{T_D}}{2\delta} {t_D}^{1/4}. \tag{11}$$

Note that Eq. (11) is written in the notation used in this paper. $f(t_D)$ represents a function that describes the transient behavior of pressure in the well and δ denotes a constant.

2.4 Description of the model setup

We ran the numerical simulations in the Subsurface Flow Module of COMSOL Multiphysics® software program. The space- and time-dependent balance equations, described in section 2.1, together with their initial and boundary conditions are numerically solved in the entire modeling domain employing the finite-element method (FEM) in a weak formulation. The discretization of the partial differential equations (PDEs) results in a large system of sparse linear algebraic equations, which are solved using the linear system solver MUMPS (MUltifrontal Massively Parallel Sparse direct Solver), implemented in the finite element simulation software COMSOL Multiphysics®. Utilizing the Galerkin approach, Lagrange quadratic shape functions have been selected to solve the discretized diffusivity equations for the pressure process variable. For the time discretization, a Backward Differentiation Formula (BDF, *implicit method*) of variable order has been chosen.

The two-dimensional model set-up in this work is composed of a vertical fracture embedded in a confined horizontal reservoir. The matrix and fracture are porous geologic media considered saturated, continuous, isotropic, and homogeneous. The gravity effects are neglected. Fluid flow enters or abandons the matrix-fracture system only through the well. This investigation is symmetric, i.e. the flow rate calculated in the well q_w corresponds to the half of total flow rate for the case of studying the complete fracture length (see Fig. 1). The pressure in the well p_w is set to ~~10^6 Pa~~1 MPa during the entire simulation and the initial conditions for pressure in the ~~reservoir~~matrix and the fracture p_i is set to ~~10^5 Pa~~100 kPa. We use these pressure conditions in order to ensure an injection of fluid from the well to the matrix-fracture system. The order of magnitude of $(p_w - p_i)$ is similar to that utilized by Nashawi and Malallah (2007). No-flow boundary conditions are assigned to the boundaries of the reservoir since it is considered as confined. In order to ensure that the boundary conditions do not affect the modeling outcome, the system size was consecutively enlarged to double, triple, and quadruple, and the results were compared to each other and, in fact, they were identical. Additional studies have been conducted to further examine the independency of simulation results from the boundary conditions set for the simulation time considered. The pressure has been monitored at the boundary of the model for the case of imposing no-flow boundary condition (closed reservoir). No pressure variation has been detected at the boundaries of the model, which corroborates the previous observation that the simulation results have not been affected by the boundary condition set. Further, the boundary condition has been changed to constant pressure (open reservoir). Also, for this latter case, no changes were recognized in the simulation results. That way, boundary condition-independency of the solution has been guaranteed for in the computational subdomain of most interest. During the entire simulation the following parameters remained constant: $k_m = 1\ \mu D$~~$1 \cdot 10^{-18}$ m^2~~, $k_F = 1.5 \times 10^{-13}$ m^2, $s_m = 1 \times 10^{-11}$ Pa^{-1}, $b_F = 1 \times 10^{-3}$ m, and $\eta_f = 2.5 \times 10^{-4}$ Pa s. Similarly as in Ortiz R. et al. (2013), the fracture half-length takes different values from 1.5 m up to 1500 m with the objective of varying the dimensionless fracture conductivity T_D from 0.1 up to 100 (see Eq. 6). The time steps used in these numerical simulations were 0.01 s from the start until the first 40 s, 20 s from 40 s until 600 s, 60 s from 600 s until 12000 s, 300 s from 12000 s until 72000 s, 1000 s from 72000 s until 5×10^5 s, and 5×10^5 s from 5×10^5 s until 2×10^8 s (or until 6×10^8 s employed for the master curve, Fig. 2).

~~The mesh is comparatively~~ The mesh, composed of triangular elements, is relatively fine in the vicinity of the fracture and the well and it becomes gradually coarser when moving away from the fracture, since there is an extremely large hydraulic gradient near the fracture and the well (see Fig. 1b). The minimum element size is 0.0045 m near the well, the maximum element size is 80 m close to the boundaries of the reservoir, and the maximum element growth rate is 1.3 m. The number of elements varies according to the different size and mesh structure used to describe the respective model scenario. The minimum and maximum number of elements is 12,929 and 1,358,697, respectively. We performed mesh convergence studies refining the mesh, particularly, in the computational subdomain that contains steep hydraulic gradients, until the solution became mesh-independent.

3 Results

Numerical simulations ~~computed~~ show that during a~~n interval of time~~ time interval, the reciprocal of dimensionless flow rate in the well $1/q_{wD}$ is proportional to the fourth root of dimensionless time $\tau^{1/4}$ (Fig. 2). This proportionality is in accordance with the behavior documented by Guppy et al. (1981b) and Silva-López et al. (2018). In particular, we can describe the variation of dimensionless flow rate in the well during the bilinear flow regime as:

$$\frac{1}{q_{wD}}(\tau) = A \cdot \tau^{1/4}, \tag{12}$$

where the constant A ~~= 2.60~~ is equal to 2.60. From now on, we will refer to this equation as bilinear-fit-curve (grey line in Fig. 2). Note that the coefficient A obtained by Guppy et al. (1981b) employing a semi-analytical solution is approximately $A = 2.722$ (see Eq. 10). This slight difference between our and their result for A might be due to the temporal and spatial discretization utilized by them~~. This issue is discussed in the next subsection of this paper~~. The reciprocal of dimensionless flow rate exhibits a behavior proportional to the fourth root of time (Eq. 12), which is characteristic of bilinear flow regime, hence we can corroborate the occurrence of it.

We define the master curve as the one that describes the behavior of an infinitely long fracture (red line in Fig. 2). The curves describing the behavior of the reciprocal of dimensionless flow rate over time for different dimensionless fracture conductivities, from $T_D = 0.1$ up to $T_D = 100$, are addressed as type-curves (black lines in Fig. 2).

Taking into account all the aspects previously described, when type-curves start departing from the bilinear-fit-curve (Fig. 2), this indicates that the transition from bilinear flow regime to formation linear flow regime (cases with high T_D) or to pseudo-radial flow regime (cases with low T_D) begins (Ortiz R. et al., 2013).

3.1 Propagation of isobars along the fracture and the formation

In order to characterize the different isobars, the following definition is used (Ortiz R. et al., 2013):

$$P_N = \frac{p(x,y,t) - p_i}{p_w - p_i}, \tag{13}$$

where $p(x, y, t)$ denotes the pressure at the position (x, y) in the fracture or the matrix at time t. The values of P_N utilized in this study are 0.01 and 0.05, which are equivalent to the isobars of 109 kPa and 145 kPa, respectively. The isobars behave differently depending on the value of T_D. For cases with low T_D, it is distinguishable that after the termination of bilinear flow, the isobars reveal a tendency of progressing toward an elliptical or pseudo-radial flow while still propagating along the fracture (see, for example, $T_D = 0.3$ in Fig. 3 a, b, c). The lower the value of T_D, the more pronounced this tendency becomes. On the other hand, for high T_D the behavior of the isobars is similar to the formation linear flow beyond the fracture (see $T_D = 6.3$ in Fig. 3 d, e, f). Although the behavior of isobars after the termination of bilinear flow is also highly interesting, this aspect is not addressed in further detail in this work. It remains pending to be studied in a follow-up investigation.

The results of this investigation show that initially the migration of isobars P_N along the fracture (see Fig. 1) is proportional to the fourth root of time:

$$x_{iD} = \alpha_b T_D \tau^{1/4}, \tag{14}$$

where x_{iD} represents the dimensionless distance of normalized isobars P_N from the well along the x_D axis and α_b is a constant that depend~~sing~~ on the studied isobar P_N (see Fig. ~~3~~4).

In addition, the migration of isobars P_N in the matrix (perpendicular to the fracture and at $x_D = 0$, see Fig. 1) for short times may be described by:

$$y_{iD} = \alpha_m T_D \tau^{1/2}, \tag{15}$$

where y_{iD} denotes the dimensionless distance of normalized isobars P_N from the well along the y_D axis and α_m is a constant for pressure diffusion in the matrix, ~~respectively~~ that depend~~sing~~ on the isobar under investigation.

When expressing equations (14) and (15) in dimensional form, for the x axis Eq. (14) is given by:

$$x_i(t) = \alpha_b (D_b t)^{1/4}; \tag{16}$$

and for the y axis Eq. (15) is given by:

$$y_i(t) = \alpha_m (D_m t)^{1/2}. \tag{17}$$

In the Eq. (17), $D_m = k_m/(\eta_f s_m)$ ($m^2 s^{-1}$) is known as hydraulic diffusivity of matrix and is analogue to the definition of thermal diffusivity. Additionally, in the Eq. (16) $D_b = T_F^2/k_m \eta_f s_m$ ($m^4 s^{-1}$) is referred to as effective hydraulic diffusivity of fracture during bilinear flow regime (Ortiz R. et al., 2013).

The numerical results are specified as migration-type-curves (see black lines in Figs. ~~3~~4, ~~4~~5, and ~~5~~6) and the fit equations for the propagation of isobars are referred to as migration-fit-curves (see grey lines in Figs. ~~3~~4, ~~4~~5, and ~~5~~6). It can be qualitatively noticed throughout the cases under study that for low dimensionless fracture conductivities, i.e. $T_D = 0.1$ and $T_D = 0.3$, the migration-type-curves, which describe the migration of isobars P_N along both x_D and y_D axis, start departing from migration-fit-curves before the studied isobars reach the fracture tip (Figs. ~~3~~4 a, b, c, d, and Fig. ~~4~~5). In contrast, for the cases considering high dimensionless fracture conductivities, i.e. $T_D = 1.1$, $T_D = 6.3$ and $T_D = 9.4$, there is no qualitative

evidence of migration-type-curves departing from migration-fit-curves before the studied isobars P_N arrive at the fracture tip (Figs. ~~3~~4 e, f, g, h, i, j and Fig. ~~4~~5). The latter results, however, show some exceptions for a slight acceleration exhibited by the isobars P_N ~~when they are reaching~~ at times shortly before they reach the fracture tip. It is important to mention that this relatively small acceleration also occurs for cases with low dimensionless fracture conductivities (see Figs. ~~3~~4 c~~, and 3~~d). The same behavior was observed by Ortiz R. et al. (2013) for the injection at constant flow rate. The classic definition for acceleration was considered, which is the rate of change of velocity with respect to time.

~~On the one hand, when discussing qualitatively about the early time we notice that the higher the value of the isobar P_N the sooner it migrates proportional to the fourth root of time (Fig. 5)~~ On the one hand, when discussing qualitatively about the early time we notice that the higher the value of the isobar P_N the sooner it starts behaving proportional to the fourth root of time (Fig. 6). For example, at the same time ($\tau = 5 \cdot 10^{-10}$) the isobar $P_N = 0.66$ (the greater isobar under investigation) starts to migrate along the fracture proportional to the fourth root of time whereas the isobar $P_N = 0.01$ (the smaller isobar under study) has not yet started to propagate proportional to the fourth root of time. Moreover, the greater the isobar P_N the shorter its distance from the well x_{iD} in comparison to other smaller isobars when considering the same time τ, which is logical since the isobars migrate one after the other. On the other hand, when discussing qualitatively about the long time, we notice that the smaller isobar $P_N = 0.01$ departs from the migration-fit-curve when it reaches the fracture tip. In contrast, the greater isobar $P_N = 0.66$ departs from the migration-fit-curve before its arrival at the fracture tip (Fig. ~~5~~6). Additionally, it can be seen that the higher the value of isobar P_N the farthest from the fracture tip or, closer to the well, it starts departing from the migration-fit-curve. Thus, taking into consideration the migration of isobars, it is reasonable to conclude that for high dimensionless fracture conductivities T_D, the bilinear flow regime ends when the pressure front reaches the fracture tip.

Previously, we referred to the observation concerning the acceleration that isobars experience ~~when they are arriving at~~ at times shortly before they arrive at the fracture tip (see Figs. ~~3~~4~~, and 5~~6), which was also documented in Ortiz R. et al. (2013) for the case of fluid injection at constant flow rate. To prove that it is truly an acceleration, the velocity of isobars is determined by calculating $\Delta x_{iD}/\Delta\tau$ and it is graphed versus time τ as well as versus the distance of isobars from the well x_{iD} (see Fig. ~~6~~7). The existence of this acceleration in $x_{iD} = 1$ (fracture tip, see Fig. ~~6~~7) can be clearly noticed. The velocity of isobars v_{iD} during their migration along the fracture decreases almost for the complete intervals of time considered (Figs. ~~6~~7 a~~, and 6~~c), except for its evident increase at times ~~when isobars are reaching~~ shortly before the isobars reach the fracture tip. The velocity of isobars can be described within the intervals of time used as:

$$v_{iD}(\tau) = \beta_b T_D \tau^{-3/4}, \tag{18}$$

where β_b is a constant ~~depending~~ that depends on the isobar under study. The velocity of isobars in terms of their distances from well and within the ranges of distance used can be described as:

$$v_{iD}(x_{iD}) = \gamma_b T_D {x_{iD}}^{-3}, \tag{19}$$

where γ_b is a constant ~~depending~~ that depends on the isobar under study.

Before the isobars reach the fracture tip and at the same time τ, the velocity of isobar $P_N = 0.01$ is higher than the velocity of $P_N = 0.05$ (Figs. ~~6~~7 a, ~~and 6~~c). Furthermore, we can see that the arrival at the fracture tip of $P_N = 0.05$ occurs after the arrival of $P_N = 0.01$, what is also distinguishable in Figs. ~~3~~4 and ~~5~~6. The latter modeling results make sense since isobars migrate one after the other, being the smaller of them $P_N = 0.01$ first in the propagation along the fracture. Moreover, before the arrival of isobars at the fracture tip and at a certain point belonging to the fracture the velocity of the isobar $P_N = 0.01$ is higher than the velocity of $P_N = 0.05$ (Figs. ~~6~~7 b, ~~and 6~~d).

3.2 Termination of bilinear flow

~~Concerning the study related to the termination of bilinear flow considering fluid injection at constant flow rate, Ortiz R. et al. (2013) introduced three criteria: the transition criterion, the reflection criterion and the arrival criterion. The transition and reflection criteria consider data regarding the well and the arrival criterion considers data related to the migration of isobars P_N along the fracture. In this work, is presented for the first time the fracture criterion, which considers data related to the propagation of isobars along the fracture. To sum up, we can say that there exist two methodologies to quantify the termination of bilinear flow: (a) considering the transient of pressure/flow rate in the well and (b) considering the propagation of isobars P_N along the fracture.~~ Concerning the study related to the termination of bilinear flow considering fluid injection at constant flow rate, Ortiz R. et al. (2013) introduced three criteria: the transition criterion, the reflection criterion, and the arrival criterion. The transition and reflection criteria take into account measurements of flow rate in the well and the arrival criterion considers measurements of the migration of isobars P_N along the fracture. In this work, a fracture criterion is presented for the first time. This criterion quantifies the separation between the migration-type-curves and the migration-fit-curves (see Fig. 4). The time at which this separation occurs is defined as the fracture time. It is important to mention that only one criterion can be fulfilled at a time. To sum up, there exist two methodologies to quantitatively identify the termination of bilinear flow: (a) considering the transition of pressure/flow rate in the well and (b) considering the propagation of isobars P_N along the fracture. It is noteworthy that the termination time is referred to differently, according to the criterion used to identify the time at which the bilinear flow regime ceases (e.g. transition time τ_t, reflection time τ_r, arrival time τ_a, and fracture time τ_F, introduced in the subsections 3.2.1, 3.2.2, 3.2.3, and 3.2.4, respectively). Further, criteria generally aim at defining the deviation of curves obtained by numerical simulations from analytical fit curves that correspond to bilinear flow. The deviation is quantified by introducing the quantity ε (see subsections 3.2.1, 3.2.2, and 3.2.4). That is, the numerical results differ from the analytical bilinear fit curves by a value of ε due to the transition to another flow regime. Throughout the manuscript we use, for instance, $\varepsilon = 0.01$ or $\varepsilon = 0.05$ corresponding to 1% and 5% deviation, respectively. This employed notation is intended to express that when a separation between numerical results and fit curves is greater than 0.01 or 0.05, the termination of bilinear flow is evidenced.

3.2.1 Transition criterion

This criterion quantifies the clockwise deviation of type-curves from the bilinear-fit-curve in Fig. 2 and it is fundamentally utilized for low dimensionless fracture conductivities of $T_D = 1.1$ down to $T_D = 0.1$:

~~$$\varepsilon = 1 - \left(\frac{\frac{1}{q_{wDt}}}{\frac{2.60\tau^{\frac{1}{4}}}{}} \right), \quad (20)$$~~

$$\varepsilon < 1 - \left(\frac{log\left(\frac{1}{q_{wDt}}\right)}{log(2.60\tau^{1/4})} \right), \quad (20)$$

~~where q_{wDt} represents the dimensionless flow rate of type-curves (Fig. 2). The cases that are under the study of the transition criterion are not affected by the fracture tip and the termination time is similar for all type-curves for which this criterion is applicable (see τ_t in Fig. 7).~~ where q_{wDt} represents the dimensionless flow rate q_{wD} of the specific type-curve under study (Fig. 2). Note that $1/q_{wD}$ vs. τ is associated with equation $2.60\tau^{1/4}$ in a log-log plot (bilinear-fit-curve). The cases that are under the study of the transition criterion are not affected by the fracture tip and the transition time is similar for all type-curves for which this criterion is applicable (see τ_t in Fig. 8). The transition time τ_t defines the end of bilinear flow when $1/q_w$ is no longer proportional to $t^{1/4}$.

3.2.2 Reflection criterion

~~It quantifies the counterclockwise deviation of type-curves from the master curve in Fig. 2 due to their reflection at the fracture tip (Ortiz R. et al., 2013) and it is used for high fracture conductivities:~~ The reflection criterion quantifies the counterclockwise deviation of type-curves from the master curve in Fig. 2 due to isobar reflection at the fracture tip (Ortiz R. et al., 2013). When lower isobars than the isobar under study have already reached the fracture tip, these isobars are partly reflected from the fracture tip toward the well, due to the hydraulic conductivity contrast experienced at the interphase between the fracture tip and the matrix. This hydraulic conductivity structure causes the isobar reflection at the fracture tip back toward the well and the isobar transmission further into the matrix. Thus, the propagation velocity of all isobars decelerates when they leave the fracture tip and start to propagate through the matrix. This criterion it is used for high dimensionless fracture conductivities:

~~$$\varepsilon = 1 - \left(\frac{\frac{1}{q_{wD\infty}}}{\frac{1}{q_{wDt}}} \right) = 1 - \left(\frac{q_{wDt}}{q_{wD\infty}} \right), \quad (21)$$~~

$$\varepsilon < 1 - \left(\frac{log\left(\frac{1}{q_{wD\infty}}\right)}{log\left(\frac{1}{q_{wDt}}\right)} \right), \quad (21)$$

~~where $q_{wD\infty}$ denotes the dimensionless flow rate of the master curve (Fig. 2). The cases that are under the study of this criterion are affected by the fracture tip, hence the higher T_D the shorter the termination time (see τ_r in Fig. 7).~~ where $q_{wD\infty}$ denotes the dimensionless flow rate of the master curve (Fig. 2), which describes the behavior for the case of an infinitely long fracture. The cases that are under the study of this criterion are affected by the fracture tip, hence the higher T_D the shorter the reflection time (see τ_r in Fig. 8). The reflection time τ_r refers to the time at which a first variation of pressure is evident in the fracture tip.

3.2.3 Arrival criterion

~~It represents the moment at which the isobars arrive at the fracture tip. The cases that are under the study of this criterion are affected by the fracture tip, hence the higher T_D the shorter the termination time (see τ_a in Fig. 7).~~ The arrival criterion represents the moment at which the isobars arrive at the fracture tip. The cases that are under the study of this criterion are affected by the fracture tip, hence the higher T_D the shorter the arrival time (see τ_a in Fig. 8).

3.2.4 Fracture criterion

Basically, ~~it~~ the fracture criterion ~~states~~ that the separation between the migration-type-curves and the migration-fit-curves (see Fig. ~~3~~4) is representative of the end of bilinear flow regime and it is applicable to low dimensionless fracture conductivities. In this work, the propagation along y_D is not a criterion for the termination of bilinear flow, it is only a contribution to the study of its behavior. Usually, for the analysis of bilinear flow at constant injection or production flow rate the transient wellbore pressure is studied, thus the bilinear flow occurs when the wellbore pressure is proportional to the fourth root of time (Cinco-Ley and Samaniego-V., 1981; Ortiz R. et al., 2013; Weir, 1999). Similarly, for constant wellbore pressure as in this work, the bilinear flow can be recognized by the proportionality between $1/q_{wD}$ and $\tau^{1/4}$. The fracture criterion, instead of using the transition~~ents~~ of $1/q_{wD}$ ~~it~~ quantifies the separation of migration-type-curves from migration-fit-curves (Fig. ~~3~~4) and is defined as:

~~$$\varepsilon = 1 - \left(\frac{x_{iDf}}{x_{iDt}}\right), \quad (22)$$~~

$$\varepsilon < 1 - \left(\frac{log(x_{iDf})}{log(x_{iDt})}\right), \quad (22)$$

where x_{iDt} denotes the propagation x_{iD} of migration-type-curves and x_{iDf} represents the propagation x_{iD} of migration-fit-curves. The latter have the form $\alpha_b T_D \tau^{1/4}$ (see Eq. 14 and Fig. ~~3~~4). The cases that are under the study of the fracture criterion are not affected by the fracture tip and the ~~termination~~fracture time is similar for all migration-type-curves for which this criterion is applicable (see τ_F in Fig. ~~7~~8). Summarizing, this criterion takes into consideration only the movement of isobars P_N along the fracture and not the change of $1/q_{wD}$ in the well, and it is suitable for low dimensionless fracture conductivities T_D.

In the framework of this study, when we consider the transition~~ent~~ of flow rate in the well, the criteria that can be utilized are the transition criterion (see section 3.2.1) and the reflection criterion (see section 3.2.2). When we consider the propagation of isobars along the fracture, the criteria that can be used are the arrival criterion (see section 3.2.3) and the fracture criterion (see section 3.2.4).

Despite the values for the transition criterion and the fracture criterion are different, their behaviors are similar. They present almost constant values within the range of T_D in which these criteria are applied. Note that the values of fracture criterion are always higher than the values of transition criterion. The fracture criterion can give us a reliable estimate of the termination of bilinear flow when considering the low dimensionless fracture conductivities T_D for which this criterion is applicable. The transition and fracture criteria make sense only until the isobars P_N reach the fracture tip (see Fig. ~~7~~8).

As we exposed earlier, it does not make sense to discuss about the occurrence of bilinear flow after the pressure front has already arrived at the fracture tip. Nevertheless, the results show (Fig. ~~7~~8) that the reflection time τ_r (related to the flow rate calculated in the well) is greater than the arrival time τ_a (related to the moment at which the isobars reach the fracture tip). It means that the reciprocal of dimensionless flow rate calculated in the well is proportional to the fourth root of time even when the pressure front has already reached the fracture tip. ~~This aspect is discussed afterward in a subsequent section in more detail.~~

4 Discussion

The dimensionless time was not defined using the conventional definition t_{D}, but a modified definition τ presented by Ortiz R. et al. (2013). It turned out to be convenient in terms of interpreting the results for bilinear flow since it was possible to graph the behavior of $1/q_{wD}$ vs. τ for all dimensionless fracture conductivities T_D in the same graph (Fig. 2).

As for the comparison between the coefficient $A = 2.60$ obtained by us (Eq. 12) and the coefficient $A = 2.772$ documented by Guppy et al. (1981b), we can observe a discrepancy between these~~both~~ results of approximately 6%. This discrepancy can be considered rather low. ~~This difference could be attributed to the spatial and temporal discretization utilized in our work, which is more sophisticated than the discretization used by Guppy et al. (1981b).~~

Some type-curves bend clockwise and some other bend counterclockwise from bilinear-fit curve (Fig. 2). Among the cases of dimensionless fracture conductivities T_D studied, the type-curves that bend clockwise are $T_D = 0.1$, 0.3 and 1.1, and those that bend counterclockwise are $T_D = 3.1$, 6.3, 9.4, 20, 31, 50, and 100. Similar results were obtained by Ortiz R. et al. (2013) for the case of injection at constant flow rate. For the interval of time utilized in the simulation, the behavior of $1/q_{wD}$ versus τ for dimensionless fracture conductivities $T_D = 0.1$ and 0.3 is identical to the behavior of an infinitely long fracture (master curve, red line in Fig. 2) since the separation of the mentioned type-curves from the master curve shall occur at time greater than the simulation time utilized here.

Our results concerning the propagation of isobars along the fracture and the matrix (Eqs. 14, and 15) are similar to the results previously presented by Ortiz R. et al. (2013) regarding the migration of isobars. The values of α_b obtained by us for $P_N = 0.01$ and 0.05 are quantitatively different from the values documented by them in 4.6% and 5.8%, respectively.

At times when isobars are reaching shortly before the isobars reach the fracture tip, they exhibit an acceleration along the fracture (see Figs. 34, and 56). Subsequently, after arriving at the fracture tip, their progress along the fracture keep relatively constant. Subsequently, once the isobars arrive at the fracture tip, they no longer progress through the matrix over a certain period of time. Afterward, they experience another acceleration along the fracture with which the migration of isobars seems to approach to a propagation proportional to the square root of time (see Fig. 34). An identical behavior was observed by Ortiz R. et al. (2013) and they attributed it to the reflection of isobars at the fracture tip, which makes sense and could be confirmed in this study. The acceleration nearby the fracture tip can be observed more clearly when analyzing the velocity along the fracture (see Figs. 67 b, and 67d). During the intervals of time used, the migration of isobars along the fracture experiences a constant deceleration, except when they approach to the fracture tip. This deceleration is qualitatively identical for $P_N = 0.01$ and $P_N = 0.05$ (see Figs. 67 a, and 67c). It is evident that for all fixed dimensionless positions in the fracture and considering the same dimensionless fracture conductivity T_D, the velocity v_{iD} is higher for low values of normalized isobars p_N (see Figs. 67 b, and 67d). One reason of this observation is that once the deceleration begins, $P_N = 0.01$ propagates faster than $P_N = 0.05$ since the initial velocity (when the isobar leaves the well) of the isobar $P_N = 0.01$ is higher than initial velocity of the isobar $P_N = 0.05$. This behavior is explained based on the fact that the pressure gradient between the well and the fracture is bigger when $P_N = 0.01$ is leaving the well than when $P_N = 0.05$ is leaving it. Furthermore, for all fixed dimensionless positions in the fracture and considering the same isobar P_N, the velocity v_{iD} is higher for high dimensionless fracture conductivities (see Figs. 67 b, and 67d).

Using Eq. (18) and Eq. (19) the migration of isobars along the fracture can be described as:

$$x_{iD} = \left(\frac{\beta_b}{\gamma_b}\right)^{-1/3} \tau^{1/4}. \tag{23}$$

Note that Eq. (23) has the same form that Eq. (14), thus:

$$\left(\frac{\beta_b}{\gamma_b}\right)^{-1/3} = \alpha_b T_D. \tag{24}$$

It is possible to verify the validity of Eq. (24) by introducing the required values.

For the case of injection at constant flow rate the results obtained by Ortiz R. et al. (2013) for the arrival time, the reflection time, and the transition time, are similar to ours (see Table 1). It is worth noting that when using the expression ε and $P_N = 0.01$, it means that we are studying the case of the isobar $P_N = 0.01$ and we are considering that for values of ε greater than 0.01, the bilinear flow ends. Note further that when considering ε and $P_N = 0.05$, we are studying the isobar $P_N = 0.05$ and we are using a value of $\varepsilon = 0.05$ to determine the termination of bilinear flow, for all pertinent criteria.

When it comes to the criteria that consider the transitionient of $1/q_{wD}$ some observations can be made: (a) in the case of Fig. 78a the transition criterion is fulfilled up to a value of T_D approximately 2 and for values of T_D above 3 the reflection

criterion is fulfilled; and (b) in the case of Fig. ~~7~~8b the transition criterion is fulfilled up to a value of T_D approximately 1.1 and for values of T_D above 2 the reflection criterion is fulfilled. ~~Note that for the case ε and $P_N = 0.01$ and for $2 < T_D < 3$ as well as for the case ε and $P_N = 0.05$ and for $1.1 < T_D < 2$, it is not clear what happens with the transition criterion since it seems that the values converge to the fit curve for the reflection criterion (see Fig. 7). A deeper study is required to determine more precisely what occurs within those ranges of T_D. Ortiz R. et al. (2013) concluded the same based on their work.~~ Note that for the case ε and $P_N = 0.01$ and $2 < T_D < 3$ (see Fig. 8a), it is observed that values (non-filled circles) depart from the fit-curve linked to the transition criterion and start converging toward the fit-curve associated with the reflection criterion. A similar behavior is also observed for the case ε and $P_N = 0.05$ and $1.1 < T_D < 2$ (see Fig. 8b). A comprehensive study is required to unravel more precisely what occurs within those ranges of T_D. Based on their work, Ortiz R. et al. (2013) came to the same conclusion.

Finally, there are two ways to determine the termination of bilinear flow: (I) by numerically measuring the transient flow rate in the well and obtaining the transition time τ_t for low T_D and the reflection time τ_r for high T_D, and (II) according to the migration of isobars along the fracture (not measurable in the well), obtaining the fracture time τ_F for low T_D and the arrival time τ_a for high T_D (see Table 2).

4.1 Application to well testing problems

In practical terms, when analyzing the transient flow rate in a well only the transition time τ_t and the reflection time τ_r can be determined. The transition time defines the end of bilinear flow when $1/q_w$ is no longer proportional to $t^{1/4}$, and the reflection time refers to the moment at which a variation of pressure is evident in the fracture tip. With the current field methods, it is not possible to determine the termination of bilinear flow utilizing the progress of the pressure front along the fracture, although this is more physically reasonable. Nevertheless, the fracture length can be constrained indirectly, for instance by computing the time at which the pressure arrives at the fracture tip and its relation with respect to the reflection time. The relation between the arrival time τ_a and the reflection time τ_r is given by:

$$\tau_a \cong 0.0579\tau_r \tag{25}$$

for ε and $P_N = 0.01$ (see Fig. ~~7~~8a); and

$$\tau_a \cong 0.0736\tau_r \tag{26}$$

for ε and $P_N = 0.05$ (see Fig. ~~7~~8b).

In the following, we present two artificial cases in which synthetic curves were constructed to illustrate how the measurements of the flow rate in wells during hydraulic tests at constant pressure are used to estimate or restrict the length of fractures with finite hydraulic conductivity (bilinear flow). The synthetic curves are not obtained from measurements of realistic well tests, but computed utilizing the validated porous and fracture model included in COMSOL Multiphysics® and in previous papers.

4.1.1 Case 1: high dimensionless fracture conductivities T_D

We proceed to elaborate a method to estimate the fracture length using measurements of the flow rate in the well. This is motivated by its usefulness for cases with high T_D in which the reflection criterion is applicable, i.e., provided that the isobar that is under study reaches the fracture tip while bilinear flow is still in progress. In this example, the values of the dimensional fracture conductivity T_F as well as the fracture length $2x_F$ are restricted by a synthetic curve representing the transient flow rate in the well. The synthetic curve is performed assuming that $p_w = 10^6$ Pa$1\ MPa$, $p_i = 10^5$ Pa100 kPa, $k_m = 1\ \mu D10^{-18}$ m^2, $T_F = 1.5 \times 10^{-16}$ m^3, $s_m = 10^{-11}$ Pa^{-1}, $\eta_F = 2.5 \times 10^{-4}$ Pa s, and $x_F = 23.81$ m (see Fig. 89). The procedure is described in series of steps as follows:

1. Dimensionally graphing the reciprocal of flow rate vs. time. It is worthwhile noting that the counterclockwise separation of the synthetic curve (red line) from the bilinear-fit-curve (grey line) represents the moment when is exhibited in the well the of arrival of the pressure front at the fracture tip, defining the end of bilinear flow.

2. Calculate T_F as is typically done (see, e.g., Guppy et al., 1981b), i.e., based on the slope of bilinear-fit-curve $1/q_w = mt^{1/4}$ (Eq. 12). The dimensional fracture conductivity is determined as follows:

$$T_F = \left(\frac{2.61 \eta_F^{3/4}}{k_m^{1/4} s_m^{1/4} h (p_w - p_i) m} \right)^2. \tag{27}$$

   According to this example, it is obtainedT_F is obtained as $T_F =$ 1.5×10^{-16} m^3. This value is the same as the one employed to perform the synthetic curve.

3. Read from the graph the termination of bilinear flow defined by the separation of the curve that represents the $1/q_w$ measured in the well (red curve) from the curve proportional to $t^{1/4}$ (grey curve). This time corresponds to the reflection time. In practical terms, it is considered a calculation error in the separation of 5%, which corresponds approximately to the visual estimation of the point at which boththese curves start departing from each other. In this case study, the reflection time t_r is approximately 10^4 s.

4. Introduce the value of reflection time t_r calculated in the previous step in the relation $\tau_a \cong 0.0736 \tau_r$ and obtain the arrival time of the isobars at the fracture tip. For the example at hand $t\tau_a = 736$ s.

5. Determine the value of D_b from its definition:

$$D_b = \frac{{T_F}^2}{k_m \eta_F s_m}. \tag{28}$$

   For the present case study, taking into account the example and the parameters of the simulation, it is obtainedD_b is obtained as $D_b =$ 9 m^4 s^{-1}.

6. Introduce the value of t_a, obtained at step 4, and the value of D_b, calculated at step 5, in the equation of migration of isobars along the fracture (Eq. 16) and, in this way, calculate the fracture half-length. In this case, the isobar

under study is $P_N = 0.05$, as a result the constant $\alpha_b = 2.23$. Utilizing ~~the~~ Eq. (16) ~~documented for the first time in this work~~ we have:

$$x_F = \alpha_b (D_b t_a)^{1/4}. \quad (29)$$

When introducing the corresponding values of the considered example, ~~it is obtained x_F = 20.12 m~~ x_F is obtained as 20.12 m.

7. Finally, the fracture length is approximately 40.24 m ($2x_F$). It can be noted that this result is slightly lower than 47.62 m, which is the value that denotes the real magnitude used to represent the synthetic curve. It is possible to obtain more accurate results by quantitively calculating the separation between the curves of the considered example instead of visually estimating it. ~~For instance, when calculating exactly the point at which the separation is 5% it is obtained an arrival time of 865.5 s and a fracture length of 41.9 m.~~ For instance, when calculating explicitly a counterclockwise 5% separation of the synthetic curve (red line) from the bilinear-fit-curve (grey line), an arrival time of 865.5 s and a fracture length of 41.9 m are obtained.

4.1.2 Case 2: low dimensionless fracture conductivities T_D

In the case of low T_D, it is not possible to estimate the fracture length utilizing the bilinear flow theory, since this flow regime ends before the isobar at study arrives at the fracture tip. This is expressed in terms of the pressure field by the observation of the premature occurrence of a significant pressure change in the fracture tip. However, it is possible to restrict the minimum fracture length. In the following example, the values of the dimensional fracture conductivity T_F as well as the minimum fracture length $2x_F$ are constrained by a synthetic curve representing the transient flow rate in the well. This latter curve is computed assuming that $p_w =$ ~~10^6 Pa~~1 MPa, $p_i =$ ~~10^5 Pa~~100 kPa, $k_m = 1$ μD~~10^{-18} m^2~~, $T_F = 1.5$~~-~~$\times 10^{-16}$ m^3, $s_m = 10^{-11}$ ~~-~~Pa^{-1}, $\eta_F = 2.5$~~-~~$\times 10^{-4}$ Pa s, and $x_F = 136.36$ m (see Fig. ~~9~~10). The procedure is outlined in the following steps:

1. Dimensionally graphing the reciprocal of flow rate vs. time.

2. Calculate the value of T_F as commonly conducted in the related literature (See, e.g., Guppy et al., 1981b), i.e., based on the slope of bilinear-fit-curve $1/q_w = mt^{1/4}$ (Eq. 12). The dimensional fracture conductivity is determined as follows:

$$T_F = \left(\frac{2.61 \eta_F^{3/4}}{k_m^{1/4} s_m^{1/4} h (p_w - p_i) m} \right)^2. \quad (30)$$

According to this example, T_F is obtained as ~~it is obtained T_F =~~ 1.5~~-~~$\times 10^{-16}$ m^3. This value is the same as the one used to calculate the synthetic curve.

3. Read from the graph the termination of bilinear flow defined by the clockwise separation of~~f~~ the curve that represents the $1/q_w$ measured in the well (blue curve) from the curve proportional to $t^{1/4}$ (grey curve). This time is

defined as transition time and it is similar for all cases with low T_D. Similar to the previous case, a calculation error in the separation of 5% is considered, which corresponds approximately to the visual estimation of the point at which both curves start departing from each other. In this example, the transition time t_t is approximately 10^6 s.

4. Introduce the value of transition time t_t, calculated in the previous step, in the relation $\tau_a \cong 0.0736\tau_t$ and obtain the fictitious arrival time of the isobars at the fracture tip. For the contemplated case example, $t\tau_a = 73600$ s.

5. Determine the value of D_b from its definition:

$$D_b = \frac{T_F^{\,2}}{k_m \eta_F s_m}. \tag{31}$$

In the context of the example at hand and considering the parameters of the simulation, D_b it is obtained as $D_b = 9$ $m^4\ s^{-1}$.

6. Introduce the value of t_a, obtained at step 4, and the value of D_b computed at step 5, in the equation of migration of isobars along the fracture (Eq. 16) and, in this way, calculate the fictitious fracture half-length. In this case, the isobar under study is $P_N = 0.05$, as a consequence the constant $\alpha_b = 2.23$. Utilizing the Eq. (16) documented for the first time in this work we have:

$$x_F = \alpha_b (D_b t_a)^{1/4}. \tag{32}$$

When incorporating the corresponding values of this example, x_F it is obtained as $x_F = 63.62$ m.

7. Finally, the minimum fracture length is approximately 127.23 m ($2x_F$), whereas the real value used to represent the synthetic curve is 272.72 m.

In the cases described previously, the practical use of Eq. (16) to constrain the length of a fracture with finite conductivity has been demonstrated by analyzing the transient behavior of flow rate in the well during a hydraulic test at constant pressure.

The expressions obtained in this work for the ending time of bilinear flow, the pressure propagation, and the bilinear diffusivity D_b, complement the limited theory that exists about data analysis from wells producing or injecting at constant pressure. The clarity and simplicity of these equations allows these to be used quickly to estaimate the length of fractures with finite conductivity. The bilinear diffusivity D_b, firstly introduced by Ortiz R. et al. (2013) for constant well flow rate and demonstrated in this work to also hold for the case of constant well pressure, could in principle be estimated in the laboratory by means of Eq. (16). In addition, this bilinear diffusivity allows, on the one hand, for a relatively uncomplicated comparison beweenbetween finite conductivity fractures. On the other hand, these equations could in one way or another be integrated into more general methods such as the transient rate analysis for the interpretation of production data. Finally, the diffusivityon equations of pressure in the matrix and the fracture (Eqs. 16, and 17) are also useful to reduce the associated risks related to induced seismicity generated by changes of pressure in fractured reservoirs or faults, as a consequence of

massive fluid injection (e.g. Shapiro, 2015; Shapiro and Dinske, 2009). By knowing and understanding the physics behind the migration of isobars it is possible to minimize the associated risks with changes in pores pressure.

5 Conclusion

~~The results of our study suggest that the reciprocal of dimensionless flow rate $1/q_{wD}$ is proportional to the fourth root of dimensionless time τ during the bilinear flow regime for the case of injection at constant pressure in the well. Previously, Guppy et al. (1981b) obtained the factor $A = 2.722$ (Eq. 10), which is slightly greater than the factor obtained here $A = 2.60$ (Eq. 12). This discrepancy is attributed to our finer spatial and temporal discretization in comparison with the discretization used by Guppy et al. (1981b).~~

~~During bilinear flow regime the migration of isobars along the fracture is described as: $x_t(t) = \alpha_b (D_b t)^{1/4}$, where $D_b = T_F^2 / k_m \eta_f s_m$ ($m^4 s^{-1}$) is defined in the same way as in Ortiz R. et al. (2013) as the effective hydraulic diffusivity of fracture during bilinear flow regime. Moreover, the migration of isobars in the matrix is given by: $y_t(t) = \alpha_m (D_m t)^{1/2}$, where $D_m = k_m / (\eta_f s_m)$ ($m^2 s^{-1}$) denotes the hydraulic diffusivity of matrix.~~

~~As for the transient of flow rate in the well, the termination of bilinear flow is given by (a) the transition time τ_t (circumferences in Fig. 7 and Eq. 20), valid for low T_D and (b) the reflection time τ_r (squares in Fig. 7 and Eq. 21), valid for high T_D.~~

~~When it comes to the propagation of isobars along the fracture, the termination of bilinear flow is given by (a) the fracture time τ_L (filled circles in Fig. 7 and Eq. 22), valid for low T_D and (b) the arrival time τ_a (triangles in Fig. 7), valid for high T_D.~~

~~Similarly as in Ortiz R. et al. (2013), it was observed that isobars accelerate when they approach to the fracture tip (Figs. 3 and 5). This acceleration was verified by studying the velocity of isobars using the graphs v_{tD} vs. τ and v_{tD} vs. x_{tD} (Fig. 6). It was concluded that for a fixed dimensionless position in the fracture x_{tD}, the velocity v_{tD} is higher for low values of normalized isobars p_N as well as for high fracture conductivities T_D (see Figs. 6b and 6d).~~

~~In a follow up study, it would be interesting to include the effect of fracture storativity and investigate, utilizing an analogue method to that discussed in this work, the behavior of a fracture with conductivity high enough to lead to fracture and formation linear flow.~~

Numerical results obtained in this work corroborated the relation of proportionality previously presented by Guppy et al. (1981b) between the reciprocal of dimensionless flow rate $1/q_{wD}$ and the fourth root of dimensionless time τ during the bilinear flow regime for the case of injection at constant pressure in the well. Guppy et al. (1981b) obtained the proportionality factor $A = 2.722$ (Eq. 10), which is slightly greater than the factor obtained here $A = 2.60$ (Eq. 12). This discrepancy may be attributed to our finer spatial and temporal discretization in comparison with the discretization used by Guppy et al. (1981b).

The most significant findings of this work are:

i) During the bilinear flow regime, the migration of isobars along the fracture is described as: $x_i(t) = \alpha_b (D_b t)^{1/4}$, where $D_b = T_F^2 / k_m \eta_f s_m$ ($m^4\ s^{-1}$) is the effective hydraulic diffusivity of fracture during the bilinear flow regime. In addition, the migration of isobars in the matrix is given by: $y_i(t) = \alpha_m (D_m t)^{1/2}$, where $D_m = k_m/(\eta_f s_m)$ ($m^2\ s^{-1}$) denotes the hydraulic diffusivity of matrix. This simulation results are in line with the study conducted by Ortiz R. et al. (2013) for the case of wells injecting/producing at constant flow rate.

ii) The termination of bilinear flow obtained from transient flow rate analysis is given by (a) the transition time τ_t (circumferences in Fig. 8 and Eq. 20), valid for low T_D and (b) the reflection time τ_r (squares in Fig. 8 and Eq. 21), valid for high T_D.

iii) From the physical point of view, it is of interest to study the propagation of isobars along the fracture, for which the termination of bilinear flow has been found in this work to be given by (a) the fracture time τ_F (filled circles in Fig. 8 and Eq. 22), valid for low T_D and (b) the arrival time τ_a (triangles in Fig. 8), valid for high T_D. However, this methodology may encounter technological obstacles in real field situations.

iv) A new methodology is presented to constrain the fracture length (section 4.1), based on the end time of the bilinear flow and using Eq. (16) that describes the spatiotemporal evolution of the isobars along the fracture during the bilinear flow regime.

v) In terms of dimensionless parameters, the time at which a specific isobar arrives at the fracture tip is dependent only on T_D (see section 3.2.3 and τ_a in Fig. 8).

Similarly as in Ortiz R. et al. (2013), it is observed that the isobars exhibit a peak of acceleration shortly before they arrive at the fracture tip (Figs. 4, 6). This acceleration was verified by studying the velocity of isobars using the graphs v_{iD} vs. τ and v_{iD} vs. x_{iD} (Fig. 7). It was concluded that for a fixed dimensionless position in the fracture x_{iD}, the velocity v_{iD} is higher for lower values of normalized isobars p_N as well as for higher dimensionless fracture conductivities T_D (see Figs. 7 b, d).

In a follow-up study, it would be interesting to include the effect of fracture storativity and investigate, utilizing an analogue method to that discussed in this work, the behavior of a fracture with conductivity high enough to lead to fracture and formation linear flow.

Author contribution

Patricio I. Pérez D. was responsible for numerical model and simulations, analysis of results, preparation of the draft, and final paper. Adrián E. Ortiz R. contributed the theoretical underpinning, presentation of results, preparation of the draft, and final paper. Ernesto Meneses Rioseco contributed the theoretical underpinning in composing the numerical model, analysis of results, and preparation of the final paper.

Acknowledgments

It was possible to complete this work only through the international collaboration between the Department of Chemical and Environmental Engineering - Universidad Técnica Federico Santa María (Chile) and the Department of Geothermics and Information Systems - Leibniz Institute for Applied Geophysics (Germany).

Competing interests

The authors declare that they have no conflict of interests.

Nomenclature

A	constant, Eq. (12)
b_F	aperture of fracture, m
c_a	coefficient of fit equation for the arrival time, Table 1 and Fig. ~~7~~8
c_r	coefficient of fit equation for the reflection time, Table 1 and Fig. ~~7~~8
c_t	coefficient of fit equation for the transition time, Table 1 and Fig. ~~7~~8
D_b	effective hydraulic diffusivity of fracture during bilinear flow regime, Eq. (16), $m^4 s^{-1}$
D_m	hydraulic diffusivity of matrix, Eq. (17), $m^2 s^{-1}$
$f(t_D)$	transient behavior of pressure in the well, Eq. (11), Pa
h	height of the open well section, fracture height, Eq. (5), m
k_F	fracture permeability, m^2
k_m	matrix permeability, m^2
p_i	initial pressure of matrix and fracture, Eq. (5), Pa
P_N	normalized pressure difference, Eq. (13)
p_w	constant injection pressure, Eq. (5), Pa
$p(x,y,t)$	pressure at the position (x,y) in the fracture or the matrix at time t, Eq. (13), Pa
q_w	flow rate in the well, Eq. (5), $m^3 s^{-1}$
q_{wD}	dimensionless flow rate in the well, Eq. (5)
q_{wDt}	dimensionless flow rate of type-curves, Eqs. (20) and (21), Fig. 2
$q_{wD\infty}$	dimensionless flow rate of the master curve, Eq. (21), Fig. 2
$q_F(x,t)$	fluid flow between matrix and fracture, $m^2 s^{-1}$
s_F	specific storage capacity of fracture, Pa^{-1}
s_m	specific storage capacity of matrix, Pa^{-1}

t	dimensional time, Eq. (7), s
t_a	dimensional arrival time, s
t_D	conventional dimensionless time, Eq. (7)
T_D	dimensionless fracture conductivity, Eq. (6)
T_F	fracture conductivity, Eq. (6), m^3
v_{iD}	dimensionless velocity of isobars along the fracture, Eqs. (18) and (19)
x, y	spatial coordinates along, normal to the fracture with origin at the well, Eqs. (8) and (9), respectively, m
x_F	fracture half-length, Eq. (6), m
x_D, y_D	dimensionless coordinates, Eqs. (8) and (9), respectively
x_{iD}, y_{iD}	dimensionless distances of isobars from the well (along the x_D and y_D axis, Eqs. (14) and (15), respectively
x_{iDf}	dimensionless propagation of migration-fit-curves, Eq. (22), Fig. ~~3~~4
x_{iDt}	dimensionless propagation of migration-type-curves, Eq. (22), Fig. ~~3~~4
α_b	constant for pressure diffusion in the fracture during bilinear flow, Eqs. (14) and (16)
α_m	constant for pressure diffusion in the matrix, Eqs. (15) and (17)
β_b	constant for velocity in the fracture depending on time, Eq. (18)
γ_b	constant for velocity in the fracture depending on space, Eq. (19)
~~Δ~~δ	constant, Eq. (11)
ε	quantification of error in the termination of bilinear flow, Eqs. (20), (21) and (22), Fig. ~~7~~8
η_f	dynamic fluid viscosity, Pa s
τ	dimensionless time, Eq. (~~5~~7)
τ_a	dimensionless arrival time, Fig. ~~7~~8
τ_F	dimensionless fracture time, Fig. ~~7~~8
τ_r	dimensionless reflection time, Fig. ~~7~~8
τ_t	dimensionless transition time, Fig. ~~7~~8

References

Arps, J.J.: Analysis of Decline Curves, Trans. AIME, 160, 228–247, https://doi.org/10.2118/945228-G, 1945.

Agarwal, R.G., Carter, R.D., Pollock, C.B.: Evaluation and Performance Prediction of Low-Permeability Gas Wells Stimulated by Massive Hydraulic Fracturing, J. Pet. Technol., 31, 362–372. https://doi.org/10.2118/6838-PA, 1979.

Barenblatt, G., Zheltov, I., Kochina, I.: Basic concepts in the theory of seepage of homogeneous liquids in fissured rocks [strata], J. Appl. Math. Mech., 24, 1286–1303, https://doi.org/10.1016/0021-8928(60)90107-6, 1960.

Basayir Hussain Mohsin Al-Lawati: Use of rate transient analysis to enhance the well perfomance of a mature gas field, Texas A&M University, 2017.

Belyadi, H., Yuyi, S., Junca-Laplace, J.-P.: Production Analysis Using Rate Transient Analysis, in: SPE Eastern Regional Meeting, Society of Petroleum Engineers, Morgantown, West Virginia, 13-15 October, https://doi.org/10.2118/177293-MS, 2015.

Berumen, S., Samaniego, F., Cinco, H.: An investigation of constant-pressure gas well testing influenced by high-velocity flow, J. Petrol. Sci. Eng., 18, 215–231, https://doi.org/10.1016/S0920-4105(97)00014-4, 1997.

Chen, H.-Y., Teufel, L.W.: A New Rate-Time Type Curve for Analysis of Tight-Gas Linear and Radial Flows, in: SPE Annual Technical Conference and Exhibition, Society of Petroleum Engineers, Dallas, Texas, 1-4 October, https://doi.org/10.2118/63094-MS, 2000.

Cinco-Ley, H., Samaniego-V., F.: Transient Pressure Analysis for Fractured Wells, J. Pet. Technol., 33, 1749–1766, https://doi.org/10.2118/7490-PA, 1981.

Cinco L., H., Samaniego V., F., Dominguez A., N.: Transient Pressure Behavior for a Well With a Finite-Conductivity Vertical Fracture, Society of Petroleum Engineers Journal, 18, 253–264, https://doi.org/10.2118/6014-PA, 1978.

Da Prat, G.: Well Test Analysis for Fractured Reservoir Evaluation, v. 27., United States, 1990.

Dejam, M., Hassanzadeh, H., Chen, Z.: Semi-analytical solution for pressure transient analysis of a hydraulically fractured vertical well in a bounded dual-porosity reservoir, J. Hydrol., 565, 289–301, https://doi.org/10.1016/j.jhydrol.2018.08.020, 2018.

Earlougher Jr., R.C.: Advances in Well Test Analysis, Henry L. Doherty series; Monograph (Society of Petroleum Engineers of AIME), v. 5., Henry L. Doherty Memorial Fund of AIME, New York, 1977.

Ehlig-Economides, C.A.: Well test analysis for wells produced at a constant pressure, Stanford, 1979.

Escobar, F.-H., Sánchez, J.A., Cantillo, J.H.: Rate transient analysis for homogeneous and heterogeneous gas reservoirs using the TDS technique, C.T.F Cienc. Tecnol. Futur., 3, 45–59, 2008.

Fetkovich, M.J.: Decline Curve Analysis Using Type Curves, J. Pet. Technol, 32, 1065–1077, https://doi.org/10.2118/4629-PA, 1980.

Gidley, J., Holditch, S.A., Nierode, D.E., Ralph W. Veatch, J.: Recent Advances in Hydraluic Fracturing, Henry L. Doherty series; Monograph (Society of Petroleum Engineers of AIME), v. 12., 1990.

Guppy, K.H., Cinco-Ley, H., Ramey, H.J.: Effect of Non-Darcy Flow on the Constant-Pressure Production of Fractured Wells, Society of Petroleum Engineers Journal, 21, 390–400, https://doi.org/10.2118/9344-PA, 1981a.

Guppy, K.H., Cinco-Ley, H., Ramey, H.J.: Transient Flow Behavior of a Vertically Fractured Well Producing at Constant Pressure, Society of Petroleum Engineers Journal, 1981b.

Guppy, K.H., Kumar, S., Kagawan, V.D.: Pressure-Transient Analysis for Fractured Wells Producing at Constant Pressure, SPE Formation Evaluation, 3, 169–178, https://doi.org/10.2118/13629-PA, 1988.

He, Y., Cheng, S., Rui, Z., Qin, J., Fu, L., Shi, J., Wang, Y., Li, D., Patil, S., Yu, H., Lu, J.: An improved rate-transient analysis model of multi-fractured horizontal wells with non-uniform hydraulic fracture properties, Energies, 11, 1–17, https://doi.org/10.3390/en11020393, 2018.

Heidari Sureshjani, M., Clarkson, C.R.: Transient linear flow analysis of constant-pressure wells with finite conductivity hydraulic fractures in tight/shale reservoirs, J. Petrol. Sci. Eng., 133, 455–466, https://doi.org/10.1016/j.petrol.2015.06.036, 2015.

Houzé, O., Viturat, D., Ole S., F.: Dynamic Data Analysis System, 2018.

Kutasov, I.M., Eppelbaum, L.V.: Drawdown test for a stimulated well produced at a constant bottomhole pressure, First Break, 23, 25–28, https://doi.org/10.3997/1365-2397.2005003, 2005.

Locke, C.D., Sawyer, W.K.: Constant Pressure Injection Test in a Fractured Reservoir-History Match Using Numerical Simulation and Type Curve Analysis, in: Fall Meeting of the Society of Petroleum Engineers of AIME, Dallas, Texas, 28 September-1 October, 1975.

Nashawi, I.S.: Constant-pressure well test analysis of finite-conductivity hydraulically fractured gas wells influenced by non-Darcy flow effects, J. Petrol. Sci. Eng., 53, 225–238, https://doi.org/10.1016/j.petrol.2006.06.006, 2006.

Nashawi, I.S., Malallah, A.H.: Well test analysis of finite-conductivity fractured wells producing at constant bottomhole pressure, J. Petrol. Sci. Eng., 57, 303–320, https://doi.org/10.1016/j.petrol.2006.10.009, 2007.

Ortiz R., A.E., Jung, R., Renner, J.: Two-dimensional numerical investigations on the termination of bilinear flow in fractures, Solid Earth, 4, 331–345, https://doi.org/10.5194/se-4-331-2013, 2013.

Pratikno, H., Rushing, J.A., Blasingame, T.A.: Decline Curve Analysis Using Type Curves - Fractured Wells, in: SPE Annual Technical Conference and Exhibition, Society of Petroleum Engineers, Denver, Colorado, 5-8 October, https://doi.org/10.2118/84287-MS, 2003.

Samaniego-V., F., Cinco-Ley, H.: Transient Pressure Analysis for Variable Rate Testing of Gas Wells, in: Low Permeability Reservoirs Symposium, Denver, Colorado, 15-17 April, 1991.

Shapiro, S.A.: Fluid-Induced Seismicity, Cambridge University Press, Cambridge, England, 1-276, 2015.

Shapiro, S.A., Dinske, C.: Fluid-induced seismicity: Pressure diffusion and hydraulic fracturing, Geophysical Prospecting, 57, 301–310, https://doi.org/10.1111/j.1365-2478.2008.00770.x, 2009.

Silva-López, D., Solano-Barajas, R., Turcio, M., Vargas, R.O., Manero, O., Balankin, A.S., Lira-Galeana, C.: A

generalization to transient bilinear flows, J. Petrol. Sci. Eng., 167, 262–276, https://doi.org/10.1016/j.petrol.2018.03.109, 2018.

Torcuk, M.A., Kurtoglu, B., Fakcharoenphol, P., Kazemi, H.: Theory and Application of Pressure and Rate Transient Analysis in Unconventional Reservoirs, in: SPE Annual Technical Conference and Exhibition, Society of Petroleum Engineers, New Orleans, Louisiana, 30 Sep.- 2 Oct., https://doi.org/10.2118/166147-MS, 2013.

Wang, M., Fan, Z., Xing, G., Zhao, W., Song, H., Su, P.: Rate decline analysis for modeling volume fractured well production in naturally fractured reservoirs, Energies, 11, 1-21, https://doi.org/10.3390/en11010043, 2018.

Wattenbarger, R.A., El-Banbi, A.H., Villegas, M.E., Maggard, J.B.: Production Analysis of Linear Flow Into Fractured Tight Gas Wells, in: SPE Rocky Mountain Regional/Low-Permeability Reservoirs Symposium, Society of Petroleum Engineers, Denver, Colorado, 5-8 April, https://doi.org/10.2118/39931-MS, 1998.

Weir, G.J.: Single-phase flow regimes in a discrete fracture model, Water Resources Research, 35, 65–73, https://doi.org/10.1029/98WR02226, 1999.

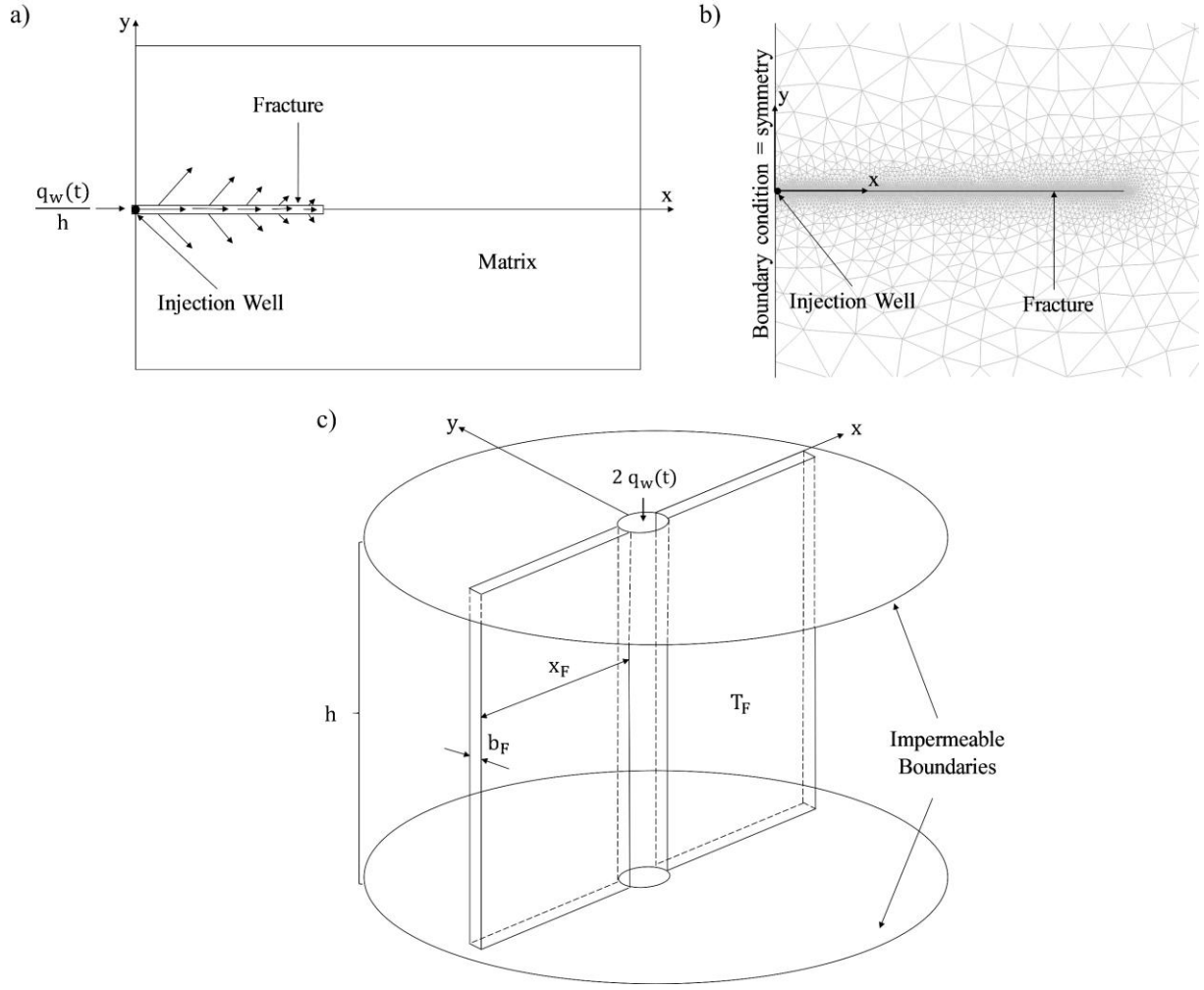

Figure 1: (a) 2D representation of model structure; (b) utilized mesh for simulation; and (c) 3D representation of model structure.

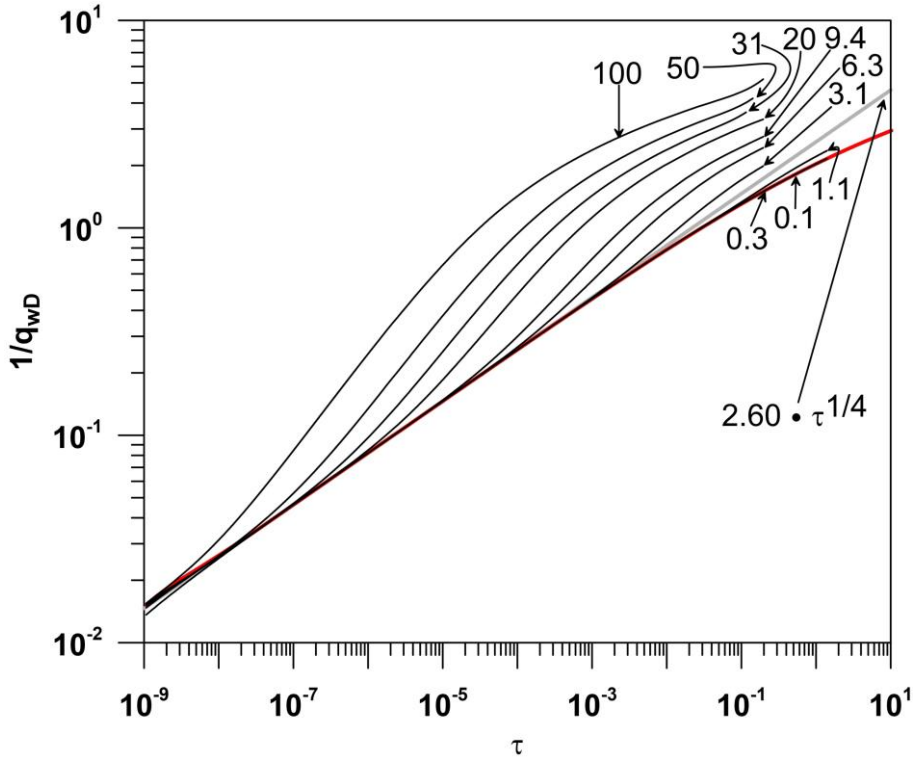

Figure 2: Model results displayed as $1/q_{wD}$ vs. τ in log-log scale. Bilinear-fit-curve (grey line), master curve (red line), and type-curves (black lines).

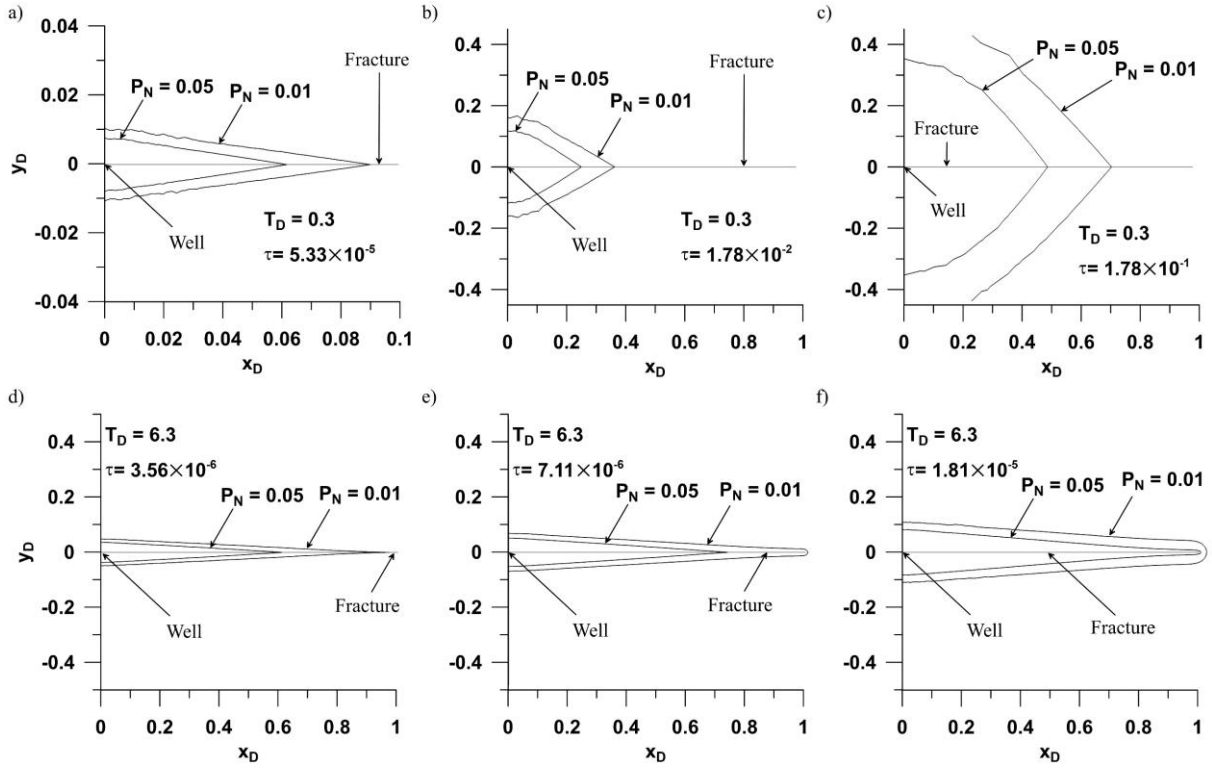

Figure 3: Spatial evolution of isobars $P_N = 0.01$ and $P_N = 0.05$ over time through the modeling domain, for the dimensionless fracture conductivities $T_D = 0.3$ (a, b, c) and $T_D = 6.3$ (d, e, f). Note that for the case of $T_D = 0.3$, the scale of the graph (a) is different from that used for the graphs (b) and (c). Read text in section 3.1 for a more detailed description of the graphs.

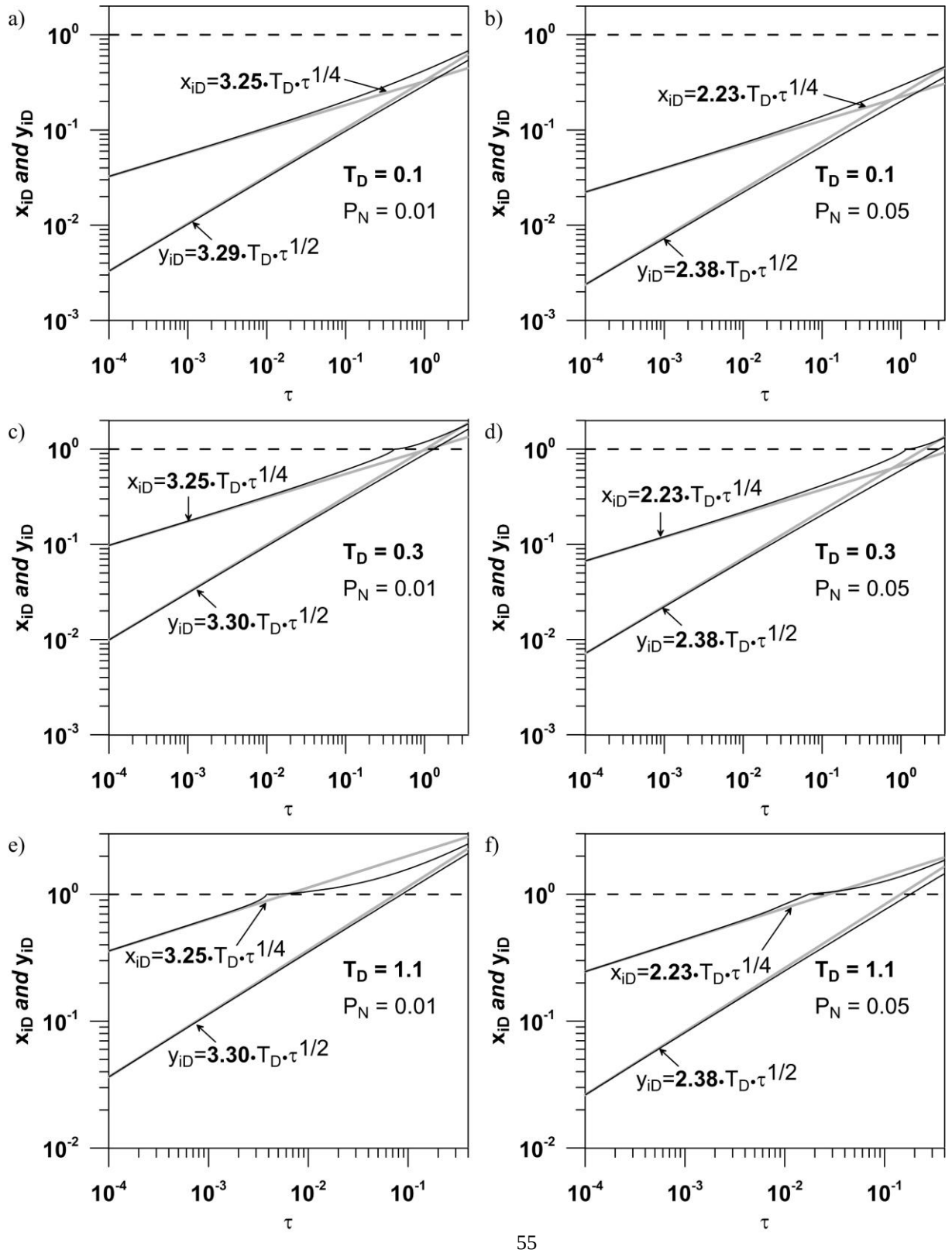
a)
b)
c)
d)
e)
f)
x_{iD} and y_{iD}
τ
$x_{iD}=3.25 \cdot T_D \cdot \tau^{1/4}$
$y_{iD}=3.29 \cdot T_D \cdot \tau^{1/2}$
$x_{iD}=2.23 \cdot T_D \cdot \tau^{1/4}$
$y_{iD}=2.38 \cdot T_D \cdot \tau^{1/2}$
$y_{iD}=3.30 \cdot T_D \cdot \tau^{1/2}$
$T_D = 0.1$
$T_D = 0.3$
$T_D = 1.1$
$P_N = 0.01$
$P_N = 0.05$

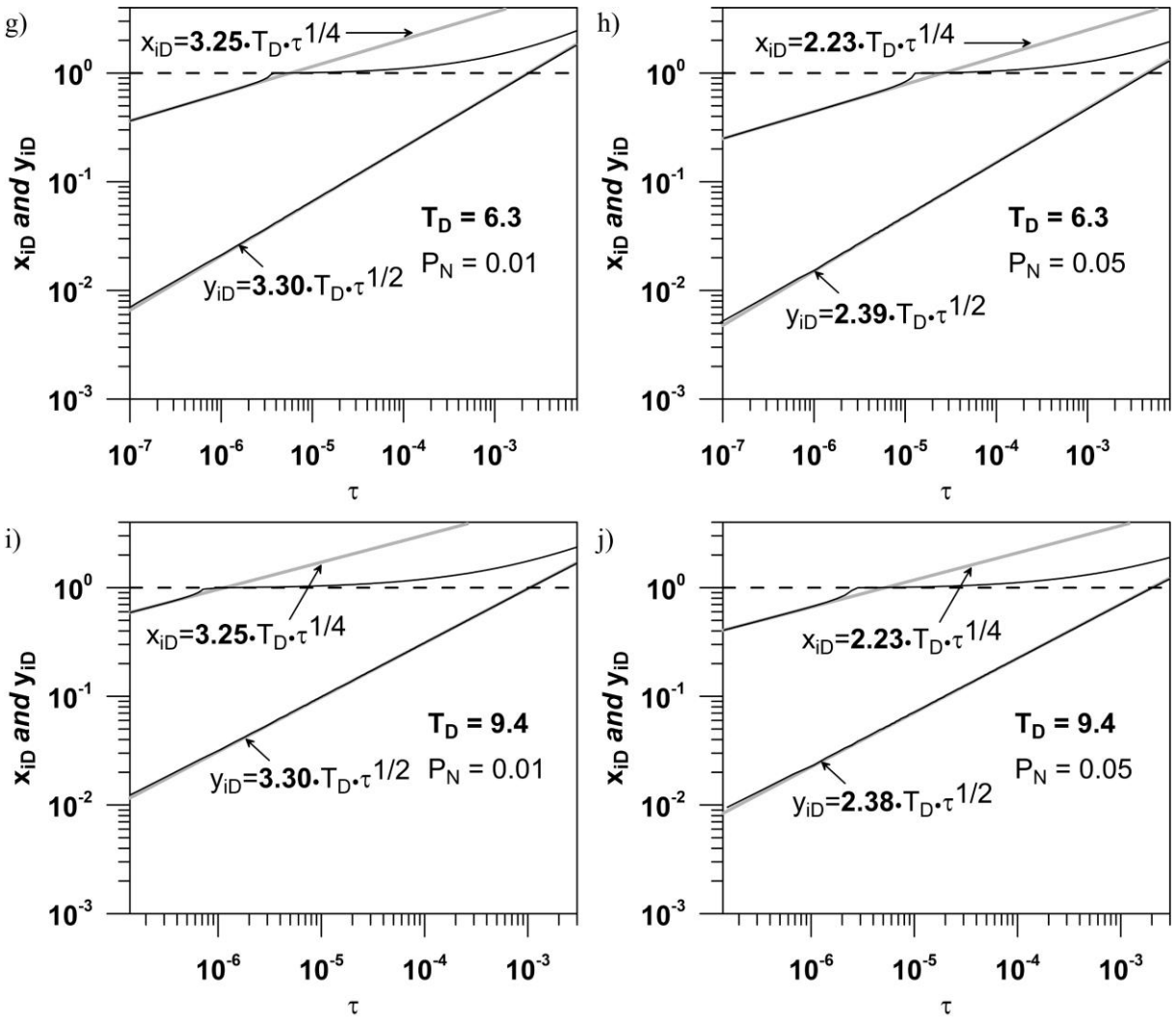

Figure ~~34~~: Model results display x_{iD} and y_{iD} vs. τ in log-log scale. Propagation of isobars $P_N = 0.01$ (a, c, e, g, i) and $P_N = 0.05$ (b, d, f, h, j) along the fracture and the formation considering the following dimensionless fracture conductivities: $T_D = 0.1$ (a, b), 0.3 (c, d), 1.1 (e, f), 6.3 (g, h), and 9.4 (i, j). The dashed lines represent the arrival at the fracture tip of the specific isobars indicated in the graphs.

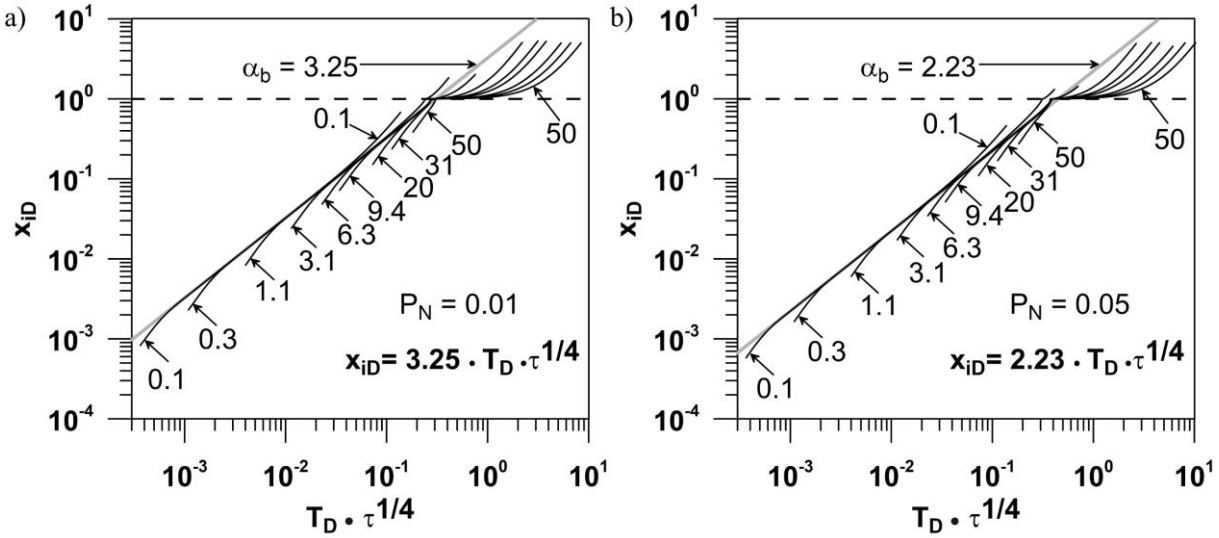

Figure 45: Model results in terms of x_{iD} vs. $T_D \cdot \tau^{1/4}$ in log-log scale. Propagation of isobars P_N along the fracture considering the following dimensionless fracture conductivities: $T_D = 0.1, 0.3, 1.1, 3.1, 6.3, 9.4, 20, 31,$ and 50. (a) Model scenarios with $P_N = 0.01$ and $\alpha_b = 3.25$; (b) model scenarios with $P_N = 0.05$ and $\alpha_b = 2.23$. The dashed lines represent the arrival at the fracture tip of the specific isobars indicated in the graphs.

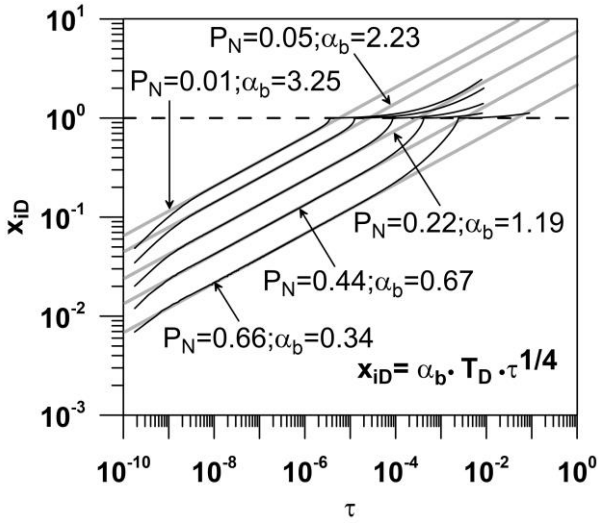

Figure 56: Modeling results in terms of x_{iD} vs. τ in log-log scale. Propagation of isobars $P_N = 0.01, 0.05, 0.22, 0.44$, and 0.66 with $T_D = 6.3$. The dashed line represents the arrival at the fracture tip of the specific isobars indicated in the graph.

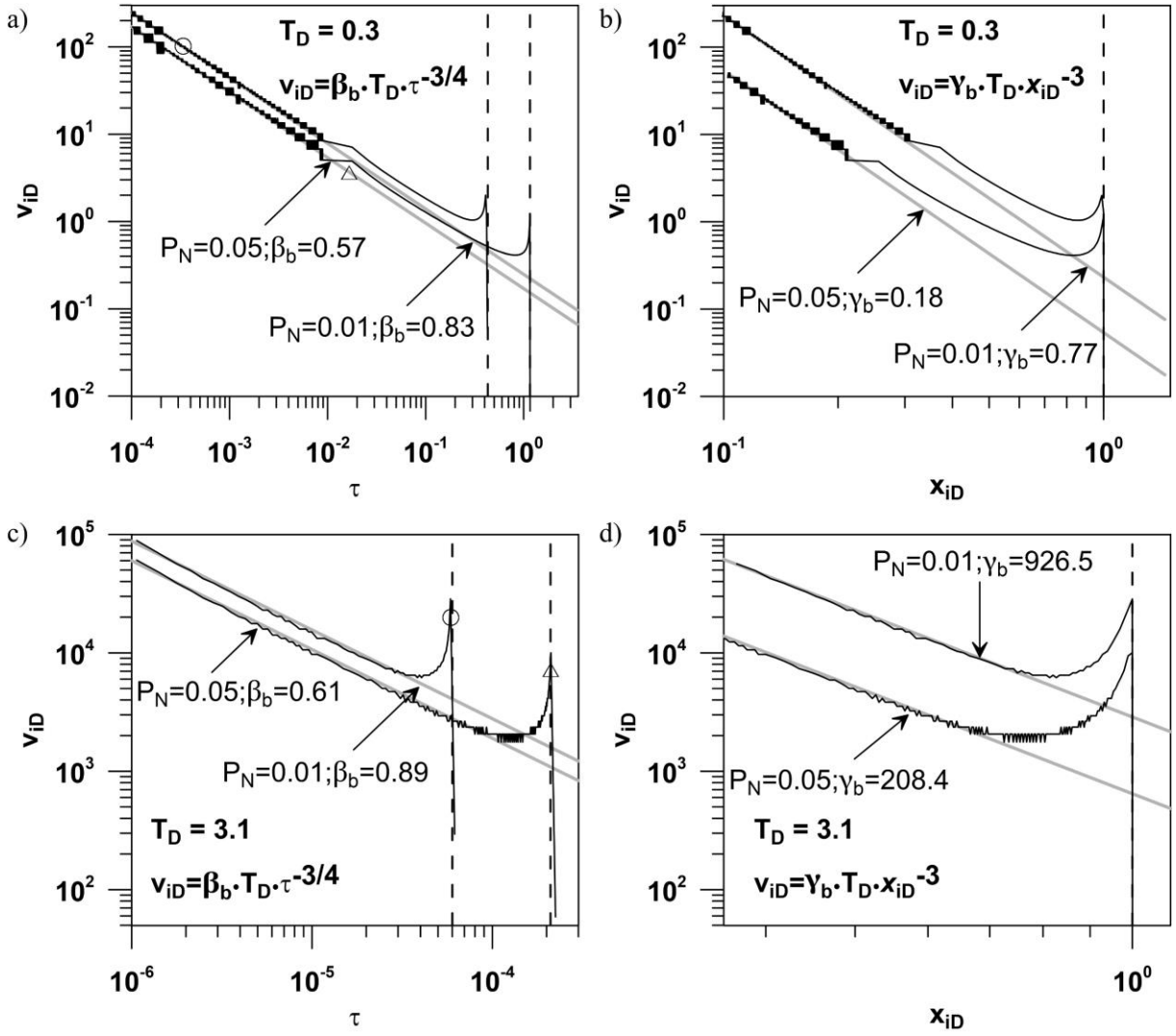

Figure ~~6~~7: Model results showing v_{iD} vs. τ and v_{iD} vs. x_{iD} in log-log scale. Velocity of isobars $P_N = 0.01$ and 0.05 considering $T_D = 0.3$ (a, b) and 3.1 (c, d). The dashed lines represent the arrival of the specific isobars at the fracture tip. (a) The circle and triangle symbols represent the transition time τ_t for $P_N = 0.01$ and 0.05, respectively (see Eq. 20). (c) The circle and triangle symbols represent the arrival time τ_a for $P_N = 0.01$ and 0.05, respectively (see Fig. ~~7~~8).

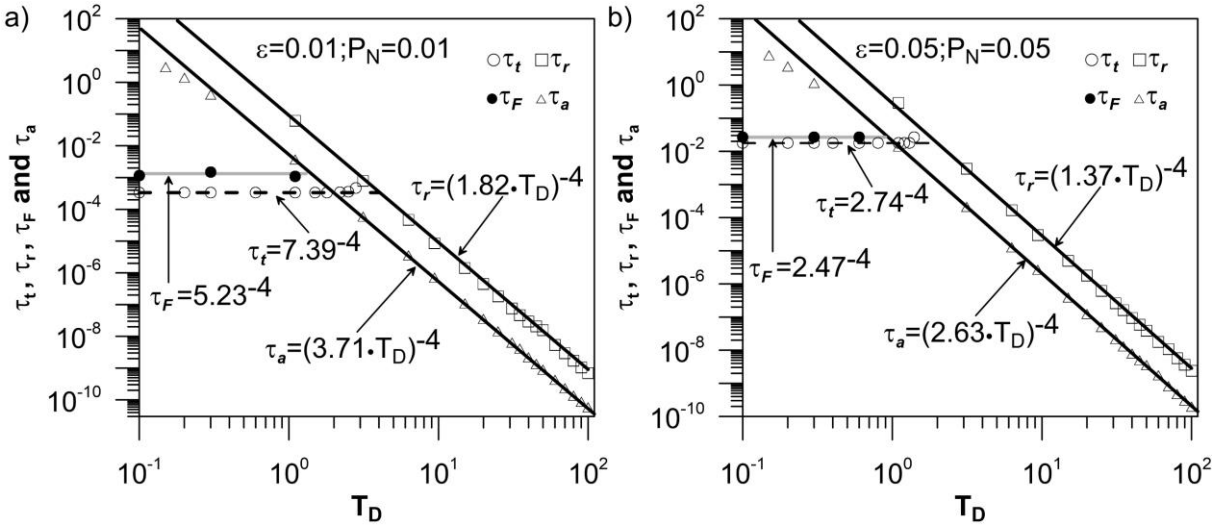

Figure ~~7~~8: Model results displaying τ_t, τ_r, τ_F, and τ_a vs. T_D in log-log scale. τ_t, τ_r, τ_F, and τ_a denote the transition time, the reflection time, the fracture time, and the arrival time, respectively. The fit-curves for reflection time and arrival time are represented by black lines, for transition time by dashed lines, and for fracture time by grey lines. (a) Numerical simulations with ε and $P_N = 0.01$; and (b) numerical simulations with ε and $P_N = 0.05$ (see Eqs. 20, 21 and 22).

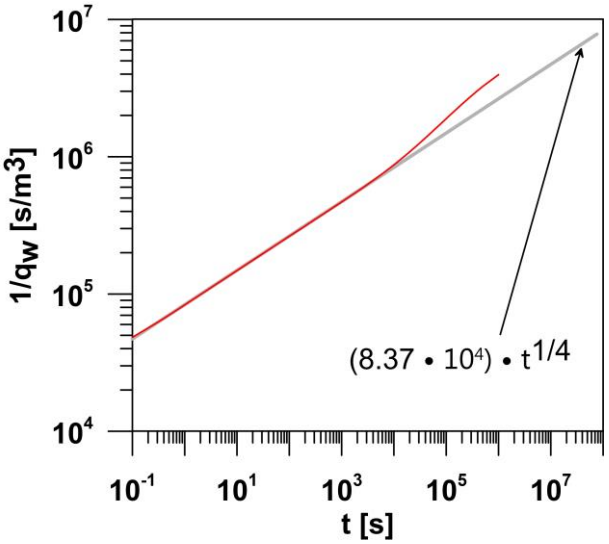

Figure ~~89~~: $1/q_w$ (s m^{-3}) vs. t (s) in log-log scale. The synthetic curve is represented by the red line and the bilinear-fit-curve is displayed with the grey line.

1740

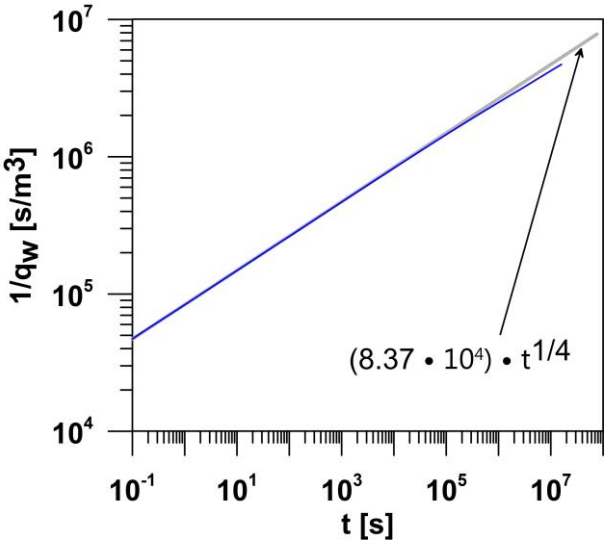

Figure ~~9~~10: $1/q_w$ (s m^{-3}) vs. t (s) in log-log scale. The synthetic curve is represented by the blue line and the bilinear-fit-curve is indicated with the grey line.

1745

Paper	Coefficient	With ε and $P_N = 0.01$	With ε and $P_N = 0.05$
Ortiz R. et al. (2013)	c_a	3.40	2.49
	c_r	1.73	1.25
	c_t	6.44	2.53
This work	c_a	3.71	2.63
	c_r	1.82	1.37
	c_t	7.39	2.74

Table 1: Comparison of coefficients of fit equations for the arrival time, the reflection time, and the transition time, which have the form $\tau_a = (c_a \cdot T_D)^{-4}$, $\tau_r = (c_r \cdot T_D)^{-4}$, and $\tau_t = (c_t)^{-4}$, respectively (see Fig. 8).

1750

Case	Termination time	With ε and $P_N = 0.01$	With ε and $P_N = 0.05$
I	τ_t	$T_D < 2$	$T_D < 1.1$
	τ_r	$T_D > 3$	$T_D > 2$
II	τ_F	$T_D < 1.2$	$T_D < 0.9$
	τ_a	$T_D > 1.2$	$T_D > 0.9$

Table 2: Criteria utilized to calculate the termination of bilinear flow. See discussion for the definition of the case I and II.